UNCLASSIFIED
RESTRICTED

Copy
RM E50D03a

NACA
RM-E50D03a

NACA RM E50D03a

NACA CASE FILE COPY

RESEARCH MEMORANDUM

HEAT-TRANSFER AND OPERATING CHARACTERISTICS OF ALUMINUM FORCED-CONVECTION AND STAINLESS-STEEL NATURAL-CONVECTION WATER-COOLED SINGLE-STAGE TURBINES

By John C. Freche and A. J. Diaguila

Lewis Flight Propulsion Laboratory
Cleveland, Ohio

NATIONAL ADVISORY COMMITTEE
FOR AERONAUTICS

WASHINGTON
June 30, 1950

RESTRICTED

JUL 14 1950

NATIONAL ADVISORY COMMITTEE FOR AERONAUTICS

RESEARCH MEMORANDUM

HEAT-TRANSFER AND OPERATING CHARACTERISTICS OF ALUMINUM FORCED-CONVECTION AND STAINLESS-STEEL NATURAL-CONVECTION WATER-COOLED SINGLE-STAGE TURBINES

By John C. Freche and A. J. Diaguila

SUMMARY

Two water-cooled turbines, one of aluminum alloy utilizing the principle of forced-convection cooling and the other of stainless steel utilizing the principle of natural-convection cooling, were operated to obtain heat-transfer and general operating data, such as blade temperatures, coolant-flow rates, and coolant pumping losses.

The outside heat-transfer results obtained on the forced-convection water-cooled aluminum turbine rotor blades agreed within 10 percent for the range of data covered with the results of two separate static-cascade investigations. The inside heat-transfer results for the aluminum-turbine rotor blades deviated from investigations made for the fully developed laminar flow of heated liquids through stationary tubes by a maximum of 40 percent for most of the data; a mean through the stainless-steel-turbine stator data deviated 15 percent from these stationary-tube investigations. The inside heat-transfer data for the steel-turbine rotor blades showed agreement with the general law describing natural-convection heat transfer; that is, Nusselt number is a function of Grashof and Prandtl numbers.

The experimentally obtained coolant pumping power for the aluminum turbine coincided with theoretical values calculated on the basis of rate of change of moment of momentum of the coolant; for the steel turbine, the experimental values exceeded the calculated values, probably because of variations in the readings, coolant leakage, and frictional resistance in the passages. Coolant pumping losses on both turbines are reducible by discharging the coolant at a smaller radius than was done in these experimental turbines.

INTRODUCTION

Turbine inlet-gas temperatures are limited because of stress limitations in current high-temperature materials. High inlet-gas temperatures result in substantial increases in the power output of both turbojet and turbine-propeller power plants. The development of improved materials has raised the inlet-gas temperature limit within the past few years, but cooling, particularly liquid cooling, promises large increases in turbine operating temperatures.

Experimental cooling work on rotating turbines at the NACA Lewis laboratory is being directed towards the following three principal objectives: (1) to understand and to evaluate quantitatively the laws governing the basic heat-transfer and flow phenomena in and around cooled turbine blades; (2) to provide operational data on the effectiveness of various blade-cooling methods and configurations; and (3) to evaluate the laws governing the performance characteristics of cooled turbines.

The known methods for determining the heat-transfer characteristics of turbines with cooled blades are presented in references 1 and 2. Some of the methods expressed in these reports have yet to be verified experimentally as was attempted in this investigation.

Experimental data obtained from two single-stage water-cooled turbines in an investigation conducted at the NACA Lewis laboratory are presented herein. The data from a forced-convection water-cooled aluminum turbine includes average convection heat-transfer coefficients outside the rotor blades and in the coolant passages. The data from a natural-convection water-cooled stainless-steel turbine includes average convection heat-transfer coefficients inside the rotor- and stator-blade coolant passages. The pumping power and the pertinent operating data, such as blade temperatures and coolant-flow rates, are presented for both turbines. In addition, the difficulties that were encountered in sealing the rotor coolant on the steel turbine are discussed. The over-all cooling losses or over-all turbine performance were not determined.

The two turbines with which these data were obtained differ primarily in the method of rotor-blade-coolant circulation employed, in the type of turbine-rotor material used, and in the blading configuration. The aluminum turbine utilized forced-convection circulation of the rotor-blade coolant and the passages were interconnected at the blade tip to provide a continuous passage for the

coolant through the blades; the stator blades were uncooled. The stainless-steel turbine employed natural convection for the circulation of the rotor-blade coolant. The passages were not interconnected; therefore coolant flowed to the blade tip and back to the root in the same passages. The stator blades were cooled by forced convection.

FORCED-CONVECTION WATER-COOLED ALUMINUM TURBINE

Apparatus

A single-stage forced-convection water-cooled aluminum turbine was operated to obtain experimental data on the effectiveness of forced-convection cooling. Blade, disk, and installation are shown in figure 1.

Turbine rotor. - The turbine rotor, which has a tip diameter of 12.06 inches, consists of two disks machined from 14S-T aluminum alloy. The 50 impulse blades with a 0.744-inch chord, 1.15-inch span, constant cross section, and no twist were integrally machined with one of the disks. In order to facilitate machining, the blades were untapered and were cut as a series of planes and cylinders. Into each blade were drilled four radial coolant passages and two transfer passages connecting the coolant passages at the tip of the blade. The outside ends of the coolant passages were sealed with screwed-in aluminum plugs. The radial coolant passages were of two diameters; those nearest the leading and trailing edges of the blades were 0.062 inch and those nearest the blade center were 0.099 inch. The diameter of each transfer passage was 0.062 inch.

The path of the coolant through the turbine is shown in figures 1(a) and 1(c). The cooling water entered the turbine shaft through a stationary tube, flowed through holes drilled in the shaft into the space between the turbine disk and the baffle plate separating the incoming and outgoing coolant, flowed radially outward through the two coolant holes nearest the blade leading edge, across the blade tip through the transfer passages, and radially inward through the two passages nearest the blade trailing edge. The coolant was discharged through axial passages drilled through one of the turbine disks into a collector formed by the inner wall of the exhaust hood from which it was emptied into the gas stream.

Rig. - The rotor was installed in a test rig built around an uncooled commercial turbosupercharger nozzle box, bearings, and bearing housing. The turbine power was absorbed by a cradled

high-speed water brake. Prior to entering the turbine, the coolant was passed through a chemical water-softening system that reduced ionizable solids in the water to below ten parts in a million. As an added precaution, two commercial cloth and wire filters were placed in series in the galvanized cooling-water pipe line upstream of the turbine.

Hot-gas system. - The induction system consisted of a variable-size orifice for air-flow measurement, an air filter, two commercial-type burners, and a straight section of pipe to allow thorough mixing of the products of combustion before they entered the turbine. The burners were supplied with air from the laboratory combustion-air supply system. The exhaust ducting and the manner of discharging the exhaust gas were the same as those described in reference 3.

Instrumentation. - Previous operation of this turbine indicated that the total-pressure loss varied at several positions around the stator-ring circumference, and in a radial direction through each stator-blade passage. The installation of three or four pressure rakes at equal intervals about the stator-ring circumference would therefore be insufficient to give a true indication of the actual average pressures. Prior to the installation of the turbine rotor, an extensive nozzle-box survey was made at inlet-gas temperatures from 70° to 1400° F, inlet pressures of 30 and 38 inches of mercury absolute, and pressure ratios from the critical value to 1.2. From these data, the total-pressure loss was averaged over the stator-ring circumference at several radial stations. A relation was obtained from these data that permitted correlation with the readings obtained during turbine operation. This method permitted a closer approximation of the average gas state at the stator outlet and more accurate heat-transfer calculations.

The survey mechanism consisted of a total-pressure rake and a thermocouple rake connected to a synchronous motor drive through reduction gears that caused the rakes to rotate at 1/20 rpm. At this slow speed, the pressure fluctuations registered by the probes passing the stator blades were recorded on a pressure recorder. The temperature changes were recorded by an automatic potentiometer. With the selected speed of travel, the circumferential temperature gradient was sufficiently small to cause a negligible error due to thermocouple lag.

The survey points covered a range broad enough to establish a relation between the readings from the stationary instrumentation at the stator inlet and throat and the survey readings at the stator outlet that would be applicable to anticipated turbine operation.

Only three blades were instrumented, two thermocouples to a blade, to indicate blade-metal temperatures at various points. Locations of four of the six thermocouples on the rotor blades are indicated in figure 1(a). At the pitch diameter, thermocouples were located at the leading and trailing edges, and at points on the pressure and suction surfaces, approximately midway between the leading and trailing edges. In addition, a thermocouple was located at the center of the pressure surface at the blade tip and another at the center of the suction surface at the blade root. A thermocouple on the water-outlet side of the baffle plate indicated the water temperature immediately prior to its discharge from the rotor. These temperatures were read from a potentiometer by means of a rotating thermocouple pick-up consisting of a slip-ring and brush system. The thermocouple leads to the pick-up extended through the hollow shafts of the turbine and water brake.

The planes of instrumentation through the rig are shown in figure 1(c). In the vertical duct upstream of the inlet collector, a rake of five unshielded thermocouples and six total-pressure tubes extended across the passage. From the center of the passage, the thermocouples were located at zero radius, and at each of two radii, approximately 5/8 and 7/8 of the duct radius. Total-pressure tubes were located at radii approximately 1/2, 3/4, and 7/8 of the duct radius. Four static-pressure wall taps were spaced 90° apart in the same plane. In addition, a thermocouple shielded by three concentric cylinders and a platinum-shielded thermocouple developed by the National Bureau of Standards were installed to measure gas conditions in a plane 1/2 inch upstream of the first instrumentation plane (not shown in fig. 1(c)). This instrumentation was inserted to determine whether any radiation error existed in reading the unshielded thermocouples. Four Bureau of Standards platinum-shielded thermocouples were installed immediately upstream of the stator blades, approximately 90° apart around the stator-ring circumference. At the throat of each of three stator-blade passages spaced 120° around the stator ring, static pressures were measured at the inner and outer radius of the flow annulus as well as on the midspan point of the suction surface of a stator blade. A single total pressure was measured at the pitch diameter at the throat of each of these three passages. Three stator-blade temperatures (root, pitch line, and tip) were measured at each of three stator blades adjacent to those on which the pressure instrumentation was located. By means of this instrumentation, the pressure loss through the nozzle box could be determined and used to obtain the gas state at the stator outlet.

The gas total temperatures and total pressures were measured 3 chord lengths downstream of the rotor by three shielded thermocouple rakes and three total-pressure rakes spaced 120° apart around the flow annulus. The pressure taps and the thermocouples on these rakes were equally spaced across the flow annulus. Static pressures were taken at the outer wall of the outlet duct at the same three locations. The cooling-water inlet temperature was measured by a thermocouple in the inlet pipe just upstream of the turbine rotor. Turbine speed was measured by an electric tachometer and checked with a chronometric tachometer. Coolant flow and fuel flow were measured by rotameters. Turbine output was measured by a NACA thrust cell in conjunction with a cradled dynamometer.

Accuracy. - The accuracy of the measurements is estimated to be within the following limits:

Blade temperature, °F	±3
Gas temperature, °F	±10
Pressures, in. Hg	±0.10
Coolant-flow rate, percent	±2
Torque, percent	±1.0

Procedure

Heat-transfer runs. - In obtaining outside heat-transfer coefficients, it is desirable to operate over a wide range of gas-flow Reynolds numbers while maintaining a constant angle of attack into the rotor blades. At predetermined values of inlet-gas temperatures, pressure ratio, and turbine speed, chosen to provide a constant angle of attack into the rotor blades, the inlet-gas density was varied to give a wide range of mass flows and hence Reynolds numbers on the outside of the blade. Runs under these conditions were made at inlet-gas temperatures of 600°, 800°, and 1000° F. At a pressure ratio of 1.6, the corresponding turbine speeds were 11,500, 12,500, and 13,500 rpm, respectively.

One series of runs was made at each of the conditions described while the average blade temperature was held constant at 220° F, a safe value insofar as blade stress was concerned. A second series of runs was also made at each of the flow conditions previously described, but the average blade temperature was allowed to vary by altering the coolant flow in increments over as wide a range as possible.

The first series of runs, although planned primarily to determine the outside coefficient over a wide range of gas-stream Reynolds numbers, was used to determine the inside coefficients as well because a small range of coolant-flow Reynolds numbers was also covered. The second series provided a large range of coolant-flow Reynolds numbers for the inside-coefficient correlation. The data from the second series of runs were also used in the outside-coefficient correlation when the scatter of data due to a possible blade-stream temperature ratio was found to be slight. By this means, more points were provided on each correlation plot without excessive turbine operation.

Coolant-pumping-power runs. - A series of runs was made to determine the coolant pumping power over a range of speeds and coolant flows similar to that for the heat-transfer runs. The coolant flow was varied from 0 to 6.8 gallons per minute while the turbine was driven by cold air at speeds up to 12,500 rpm, and the torque was observed at each point setting. The torque reading at zero coolant flow was subtracted from those obtained at the different coolant flows and the pumping power was calculated from these differences.

Methods of Calculation

Heat transfer. - The average convection coefficients were determined by the basic formula

$$Q = HA\ (\Delta T) = w_l c_p\ (\Delta T_l) \tag{1}$$

(All symbols are defined in appendix A.) The outside coefficient obtained from this expression is an average of the individual coefficients to the blade, the blade tip, and the disk rim between the blades. This average value is used because the apparatus used does not provide data for separating the heat-flow quantity Q into its component parts; that is, it was impossible to determine what part of the over-all Q was absorbed by the blade coolant through the blade tip, through the lateral surface of the blade, or through the section of disk rim between the blades that is exposed to the gas stream.

The actual expression used to determine the average outside-convection coefficient is:

$$Q = H_o \left[A_B\ (T_{g,e} - T_2) + A_3\ (T_{g,e} - T_3) + A_4\ (T_{g,e} - T_4)\right] \tag{2}$$

The effective gas temperature, or the temperature effecting heat transfer at the rotor-blade inlet, was determined by

$$T_{g,e} = T_g + \Lambda \frac{W^2}{2gJc_p} \tag{3}$$

The value of the recovery factor Λ was taken as 0.85, an average value determined from reference 4. The value of blade temperature is the integrated average on the basis of surface area of the thermocouples about the blade midsection. The values of T_3 and T_4 are the temperatures indicated by the individual thermocouple at these locations.

The average inside-convection coefficient was calculated by the expression

$$Q = H_i A_i (T_B - T_{l,av}) \tag{4}$$

Correlation of the rotor outside coefficients was attempted on the basis of the general form of the equation given in reference 5

$$Nu = f\,(Re, Pr) \tag{5}$$

Fluid properties were based on the average blade-wall temperature; the density was based on the midspan rotor-inlet static pressure and the average blade-wall temperature; and the calculated relative velocity was taken as the relative velocity at the rotor inlet. Lack of static-pressure measurements around the blade surface prevented the calculation of a Reynolds number based on average pressure and velocity conditions around the blade. The characteristic dimension D in the Nusselt number was considered to be the blade perimeter divided by π.

On the inside or coolant-passage surfaces, the data were correlated by the general equation

$$Nu = C \left[(Re)(Pr) \left(\frac{D}{L} \right) \right]^a \left(\frac{\mu_l}{\mu_B} \right)^b \tag{6}$$

The term within the bracket on the right side of equation (6) is a modified Graetz number. The other term on the right side of the equation is the ratio of coolant viscosity at coolant temperature to coolant viscosity at blade temperature. The data were correlated

by this formula because most of the calculated coolant Reynolds numbers were below 2000. This type of equation is used in reference 6 to correlate the inside coefficient in fully developed laminar flow inside stationary tubes. Fluid properties were based on the average of the coolant inlet and outlet temperatures. The characteristic dimension D was taken as the hydraulic diameter (four times the sum of the passage areas divided by the sum of the passage perimeters), which resulted in the use of a fictitious coolant-passage diameter. It was necessary to use such a value because a correlation could not be based upon the diameters of the individual coolant passages without determining the exact amount of flow through each passage. Calculations to determine these flows involved many assumptions and the results obtained were inconclusive. The total blade-passage length, radially outward, across, and radially inward, was taken as the L term in equation (6).

Coolant pumping power. - The energy input to the coolant between the inlet and outlet stations when heat transfer to the coolant is neglected is equal to the rate of change in the moment of momentum of the coolant. The total coolant pumping power between two stations on the rotor is then expressed by

$$P_P = \frac{w_l \omega^2}{550\ g}\left(r_6^2 - r_5^2\right) \tag{7}$$

Because the coolant was introduced at the center of the turbine and with negligible velocity relative to the wheel, the product of the velocity and the radius at this station is zero. Equation (7) can therefore be expressed in the simplified form

$$P_P = \frac{w_l \omega^2 r_6^2}{550\ g} \tag{8}$$

Results and Discussion

Outside heat-transfer results. - Plots of the average outside heat-transfer data at three inlet-gas temperatures are shown in figure 2(a), (b), and (c). The data of all these runs plotted together are shown in figure 2(d). Least-square curves have been drawn through each group of points. In figures 2(a) and 2(b) curves with slopes of 0.82 are shown; these data were obtained over a range of ratios of stream to blade temperature from 1.33 to 1.62. Data obtained over a range of ratios of stream to blade temperature from 1.80 to 1.92 are shown in figure 2(c), resulting in a curve with a

slope of 0.76. Although far from conclusive, these data indicate a trend of decreasing slope for increasing values of the ratio of stream to blade temperature. The data of all the runs plotted together in figure 2(d) were correlated according to the general equation

$$\frac{Nu}{Pr^{1/3}} = 0.047\ Re^{0.78}$$

With the exception of two points, these data fall within 10 percent of a line represented by this equation.

A comparison of the least-square curve from all the runs (fig. 2(d)) with results obtained by two other investigators in static-cascade tests is shown in figure 3. These other data were obtained from references 4 and 7 and were reworked on the same basis as the data reported herein so that a comparison might be made. The proximity of the curves is evident. The curve representing the aluminum-turbine data shows a maximum deviation from the British data of 9.8 percent and from the NACA heated-impulse-blade data of 7.2 percent; the data in all cases agree within 10 percent. The blade shapes used in the static-cascade determinations were approximately similar to those of the aluminum rotor. The comparison is considered good when it is realized that certain gas-flow conditions in rotating turbines cannot be duplicated in a two-dimensional cascade. Before it can be concluded that static-cascade data can be applied to rotating turbines similar runs must be made on other cooled turbines over a considerably wider range of Reynolds numbers.

Inside-heat-transfer results. - The inside or blade-to-coolant heat-transfer data in figure 4 are calculated by equation (6). An average curve representing the results obtained in reference 6 for fully developed laminar flow of heated and cooled liquids in stationary tubes is also shown for comparison. The turbine data are displaced as much as 160 percent above this curve. For these runs, the viscosity-ratio effect is practically negligible because of the relatively small and almost constant difference between the blade temperature and the coolant temperature.

When the results are plotted on the basis of an unmodified Graetz number (fig. 5), the turbine data are displaced approximately 160 percent above an average curve for the fully developed laminar flow of heated and cooled liquids through stationary tubes. Comparison of the turbine data and a line representing the data for fully developed laminar flow of heated liquids through stationary

tubes shows the maximum deviation except for two points to be 40 percent. This curve is a composite of data of several investigations for this type of flow with heated liquids through stationary tubes; the data are compiled in McAdams (reference 8, fig. 88). The indicated increased rate of heat transfer may be due to natural-convection effects. An average Grashof number in which the gravity term was replaced by $\omega^2 r$ was calculated and found to be 6.0×10^{11}. Data over a sufficient range of speeds are not yet available with which to attempt a correlation on this basis, although the size of the Grashof number would tend to indicate that it may have a large effect. Entrance effects may have contributed to the upward displacement of the turbine data as compared with the data for laminar flow in tubes. Although the blade passages are continuous through the disk rim, the thickness of which is 0.438 inch, this length may be insufficient to eliminate all entrance effects. When this length is divided by the average hydraulic diameter of the holes, a ratio of 5.15 results. It is indicated in figure 15 of reference 9 that an entrance condition similar to the one obtained with the aluminum turbine and the ratio just described falls within the range of decreasing local coefficients. This fact would signify that the upward displacement of the turbine data is partly due to entrance effects.

Coolant pumping power. - Experimental data representing the coolant pumping power for this turbine and curves representing the theoretically calculated ideal pumping power are shown in figure 6. These calculations indicate the total ideal work done on the coolant as determined from equation (8). It can be seen that the curves for the theoretically calculated ideal coolant pumping power pass through the experimental data. The frictional resistance in the blade cooling passages and cooling discharge passages is therefore negligible for this turbine. The maximum calculated coolant pumping power shown on these curves is 13.0 horsepower at a turbine speed of 13,500 rpm and a coolant flow of 6.8 gallons per minute. For the same speed, this loss is reduced to 1.3 horsepower at a nominally minimum coolant flow of 0.7 gallon per minute. The coolant pumping power was also calculated in percentage of turbine-power output. For example, at an inlet-gas temperature of 1000° F, absolute inlet pressure of 38 inches of mercury, pressure ratio of 1.6, turbine speed of 13,500 rpm, and average blade temperature of 259° F, the pumping loss was found to be 5.26 horsepower or 4.38 percent of the calculated turbine-power output. The torquemeter was unavailable during the hot runs; the turbine power was therefore calculated from measured values of gas flow, temperature, and pressure. Almost the entire pumping-power loss could be recovered on this turbine if the

coolant is discharged at a radius equal to that at which it is introduced to the rotor. In the two turbines described herein, the coolant is discharged at a large radius because of the greater ease of installation. As the point of coolant discharge is brought closer to the coolant inlet, however, any frictional resistance would be increased and a compromise on the actual point of discharge might be necessary.

General operating results. - The turbine was operated without damage for 150 hours over a range of inlet-gas temperatures from 600° to 2100° F. For $2\frac{1}{2}$ hours of this time it was operated at an inlet-gas temperature of 2000° F and for 1 hour, at 2100° F. A series of typical operating points are shown in table I. Extremes in coolant flows were chosen for similar turbine-inlet conditions insofar as possible in order to obtain a greater range over which a comparison might be made. Some of this information is lacking at the higher inlet-gas temperature points. These runs (reference 3) were preliminary in nature and were made prior to the installation of the instrumentation required for a heat-transfer and performance evaluation. The maximum blade temperature, and therefore the limiting blade temperature insofar as turbine operation is concerned, occurred at the trailing edge and was in general much higher than that of the average blade temperature. The maximum and minimum differences between the trailing-edge and the average blade temperatures are 127° and 44° F, respectively. The inside heat-transfer coefficients increase with an increase in coolant flow. The maximum percentage of heat absorbed by the rotor coolant (present investigation) is not excessive, being 3.9 percent of the total heat of the fuel supplied to the turbine with a 0.450 ratio of coolant to gas flow, which hereinafter is designated coolant-flow ratio. A coolant-flow ratio of 0.208 does not show an exceptional drop in heat absorbed by the coolant nor an appreciable increase in blade average or maximum temperature. A coolant-flow ratio of 0.140, however, results in much higher blade temperatures. The trend is repeated in the other 1000° F gas-temperature run. This trend is not obvious in the 600° F gas-temperature runs. Table I indicates that an increase in the coolant-flow ratio beyond a certain point is ineffective. The gas temperatures reported herein are relatively low and coolant flows are, in many cases, high and possibly excessive due to the nature of these runs and to the desire to work at low-temperature levels during the earlier stages of the investigation.

Typical blade-temperature distribution around the midspan of the rotor blade for turbine inlet-gas temperatures from 600° to 1000° F and coolant-flow ratios ranging from 0.050 to 0.199 are shown in figure 7. These points were chosen because they represent the maximum and minimum turbine inlet-gas temperatures and a range of coolant-flow ratios. The thermocouple locations at the tip and root sections of the blade were at different points on the periphery of the blade with respect to each other, which prevented a plot of the spanwise temperature distribution of the blade. Figure 7 indicates that the trailing-edge temperature is appreciably higher than any other point around the blade periphery. The maximum blade temperature measured was 405° F at a gas temperature of 1000° F. As expected, the blade temperatures decrease with increases in the coolant-flow ratio at a constant gas temperature. The coolant-flow rate, however, had no appreciable effect on the trailing-edge temperature at high gas temperatures. At the lower gas temperatures, doubling the coolant flow decreased the trailing-edge temperature only 20° F. Over the range of gas-temperature and coolant conditions shown, the blade temperature varied about 50° F at all conditions except the trailing edge, where the temperature varied 157° F. These variations indicate that the blade trailing edge is the critical section of the blade insofar as cooling is concerned even though the gas temperatures in this portion of the blade passage are lowest and the conductivity of the aluminum blade material is many times higher than that of the commonly used heat-resistant materials.

Practical considerations. - Several considerations pertinent to the future design and the operation of liquid-cooled turbines became apparent after operation of the aluminum liquid-cooled turbine:

(1) The method of drilling the coolant passages from the blade tips and sealing them by means of screwed-in aluminum plugs is satisfactory because no evidence of leakage or deterioration was found after 150 hours of turbine operation. Such a method of drilling the coolant passages is an obvious aid in liquid-cooled-blade manufacture because of accessibility, as compared with the difficult setups, which could conceivably result if the blade were drilled from the base to the tip.

(2) A coolant system was devised that included all possible safeguards against clogging of the coolant passages. Because of deposits in the coolant passages during early operation, various safeguards were incorporated in the present coolant system.

(3) The trailing-edge blade temperatures far exceed those of any other location. Accordingly, it may be necessary to compromise with desired aerodynamic blade design and accept larger aerodynamic losses in order to realize appreciable benefits from blade cooling.

NATURAL-CONVECTION WATER-COOLED STAINLESS-STEEL TURBINE

Apparatus

A single-stage turbine of stainless steel was designed to obtain data on the effectiveness of natural-convection cooling with a heat-resistant material. Natural-convection circulation depends on the buoyant forces arising from differences in density between the heated fluid next to the passage walls and the cooler fluid in the center of the passages. The large centrifugal forces acting on the fluid in high-speed turbines result in a high rate of heat transfer at the coolant-passage surface. Rotor, stator blade, and installation are shown in figure 8.

Turbine rotor. - The turbine rotor has a tip diameter of 13.88 inches and 31 reaction blades of 1.74-inch chord and 2.44-inch span with a constant cross section and no twist. The rotor is composed of a disk and a blade ring that fit together by means of concentric circles of teeth cut on both sides of the disk and the blade ring (fig. 8(a)). Through bolts hold the two mating parts in place. The blades are machined integrally with the ring and both blade ring and disk are made of AISI 403 stainless steel.

The coolant circulation can be traced in figure 8(a). Five blind radial passages ranging in diameter from 0.060 to 0.125 inch are drilled in each blade. The coolant is introduced through two stationary jet nozzles into a cavity between the side of the disk and a plate bolted to the disk. From here it enters the disk through eight 0.094-inch-diameter transverse passages. The difference in density between the heated and the cooled liquid and the centrifugal force due to rotation causes circulation of the coolant within the blind passages. The coolant is discharged through 12 axial discharge passages, each having a diameter of 0.094 inch, into an annular collector and then into the turbine exhaust duct.

Stator blades. - The stator ring consisted of 23 cooled blades welded at the root and the tip to plates that formed annular manifolds. Each blade was water-cooled by forced convection through five drilled passages with diameters varying from 0.060 to 0.125 inch.

The coolant entered the nozzle box at two inlets on the top and the bottom of the outer manifold and was discharged through two outlets on the inner manifold.

Rig. - The coolant systems for the rotor and the stator blades are separate. No provision has been made as yet to recirculate the coolant. The water-softening system previously mentioned and several filters were used to reduce the possibility of scaling and the accumulation of solids in the rotor-blade passages. Turbine power was supplied or absorbed by an electric dynamometer. The outer surface of the collectors and other parts of the turbine casing were cooled by directed jets of cooling air to permit operation at high gas temperatures.

Hot-gas system. - The turbine was supplied with filtered air from the laboratory combustion-air supply. The air to the two counterflow burners was metered by a variable-size orifice. The hot gas supplied by the burners was introduced to the nozzle blades through a double-entry scroll-type collector designed for uniform velocity. The gases were discharged through an exhaust collector of similar design into the laboratory altitude exhaust system.

Instrumentation. - The rotor-blade instrumentation is shown in figure 8(a). Six thermocouples were located around the blade periphery at each of three sections: tip, pitch-line, and root. Only three thermocouples were installed on any particular blade. A thermocouple was also provided in one of the water-inlet and one of the water-outlet passages. An additional thermocouple was added at the blade tip and three thermocouples were located at various highly stressed sections of the disk. A thermocouple pick-up mounted on the end of the turbine shaft permitted reading of rotor-blade temperatures during operation.

The stator-blade instrumentation is shown in figure 8(b). Six thermocouples were installed around the blade periphery in three planes along the blade span, and six additional leading-edge thermocouples were provided. The temperature of the coolant flow into the blades was measured by thermocouples in both inlet supply lines to the outer manifold supplying the coolant passages. The temperature of the coolant flow from the blades was measured by thermocouples in both water outlets leading from the inner manifold.

The planes of instrumentation in the gas-flow path through the turbine are indicated in figure 8(c). Inlet-gas temperatures were measured by four shielded thermocouples spaced in equal radial increments along the blade span 90° apart in a plane 1/4 inch

upstream of the stator blades. Total pressures were measured in the same plane as the temperatures by four water-cooled probes each of which had three taps equally spaced spanwise over the blade passage. No instrumentation was provided at the outlet from the stator blades because of space limitations. A second plane of instrumentation was located 2 chord lengths downstream of the rotor blades. Gas temperatures and pressures were measured by three shielded thermocouples radially located at the blade midspan, three water-cooled total-pressure probes (four taps on each equally spaced across the annulus), and three static-pressure taps on the outer turbine casing spaced 120° apart. Thermocouples were placed at various points on the outer surfaces of the nozzle box, the inlet collector, and the exhaust collector for radiation calculations and for safe operation.

Power was measured during pumping-power runs by a wattmeter that indicated the electric-energy input to the dynamometer. Separate rotameters were used to meter the coolant flow to the rotor and the stator. Fuel flow was measured by rotameters. A variable-size orifice was used for air-flow measurements. Turbine speed was measured by an electric tachometer and checked with a chronometric tachometer.

Accuracy. - The coolant flows and the pressure readings are of the same degree of accuracy given for the aluminum turbine; however, the blade-temperature readings are estimated to be accurate within ±5° F because of larger scale divisions of the potentiometer. Variations in the wattmeter readings due to turbine-speed fluctuations, together with inaccuracies incurred by extrapolation on curves for dynamometer and gearbox losses, resulted in horsepower calculations accurate to approximately ±1/2 horsepower.

Procedure

A series of runs was made at a turbine speed of 14,000 rpm for gas temperatures from 600° to 1740° F and coolant flows from 0 to 8 gallons per minute to explore the potentialities of the turbine without attempting to approach critical operating conditions. No attempt was made to obtain heat-transfer data by a systematic control of variables. A series of pumping-power runs was also made in the same manner as for the aluminum turbine over a limited range of speeds. Coolant sealing was checked over a range of speeds up to 14,000 rpm.

Methods of Calculating Data

The data obtained during the preliminary runs were calculated for the average inside-convection coefficients for the rotor and stator blades. Coolant leakage prevented accurate calculation of the average outside-convection coefficients.

The average inside coefficients were obtained from equation (4). Correlation of the rotor-blade inside coefficients was attempted with the equation

$$Nu = C\ (Pr\ Gr)^n \tag{9}$$

The average coolant-passage length was used as the characteristic dimension in the Nusselt and Grashof numbers. The expression for the Grashof number for a rotating cooling passage requires one significant change; the centrifugal forces acting on the fluid far outweigh the force due to gravity, and the g term in the general formula must be replaced by $\omega^2 r$. The radius r is considered to be the radius to the centroid of a column of water with a length equivalent to the average coolant-passage length.

An integrated blade-temperature average based on the entire blade-surface area was used, and the coolant temperature was taken as the arithmetic average of the coolant-inlet and coolant-outlet temperatures in the calculation of the average coefficient. The coolant-outlet temperature is probably much lower than that of the coolant in contact with the blade metal in the cooling passages, but the difficulty of installing thermocouples in the very small coolant passages prevented measurements of the passage effective coolant temperature. Fluid properties were based on average coolant temperature.

The average inside stator-blade coefficients were obtained from equation (4). Because of thermocouple failures along the trailing edge, a representative metal temperature could be obtained over only the leading section of the blade. In addition, calculations indicated that 83 percent of the coolant flow passed through the three large holes. More accurate heat-transfer results could probably be obtained by confining calculations to the forward section of the blade. The term A_i was considered the total surface area of the three largest coolant passages in the blade. The average blade temperature was the integrated average of the thermocouples around the forward part of the blade where these coolant passages were located. The coolant flow through the three leading-edge

passages was calculated. By this means, the quantity of heat Q absorbed by the coolant flowing through the three leading-edge passages was obtained. The data were then compared to the average curve for heated and cooled liquids flowing with fully developed laminar flow through stationary tubes. This curve is expressed by the following formula (reference 8):

$$Nu = 1.75 \left(\frac{w_l c_p}{kL}\right)^{1/3} \tag{10}$$

Results and Discussion

Heat-transfer results. - The average inside rotor-blade convection coefficients presented in figure 9 are correlated on the basis of equation (9). This equation, which expresses the law generally used for natural-convection heat transfer, presupposes a correlation of Nusselt number as a function of Grashof and Prandtl numbers. The present data correlate according to this law and except for one point the scatter is within 30 percent of a least-square curve through the data (fig. 9). The fluid properties in this presentation were based on the average coolant temperature. The effective coolant temperature in the passage must be much higher than the average of the coolant temperatures at the rotor inlet and outlet because the mixing of the water entering the rotor with the heated water returning from the cooling passages would result in much lower coolant temperatures than actually exist in the coolant passages. Thus, the use of the measured coolant temperatures at the rotor inlet and outlet results in a greater temperature difference between the blade and the coolant than actually prevails in the coolant passages. This temperature difference is further increased by use of the blade peripheral temperature rather than the temperature around the coolant passage. If the actual temperature difference could be measured, higher coefficients as well as lower Grashof numbers would result. The coefficients obtained herein will nevertheless be usable and will permit the prediction of heat-transfer results for other operating conditions for this turbine when coolant and blade-temperature measurements are made in this manner. The specific values, however, will not be applicable to other turbines.

The average inside stator-blade heat-transfer data are compared in figure 10 with those for the aluminum-rotor blades. The vertical spread of the aluminum-turbine data is shown for the entire range. The steel-stator data have a similar vertical spread although the data fall somewhat lower. This result is understandable because

natural-convection effects should not play such a large part in the stationary steel-stator blades as in the rotating aluminum blades. The stator data have a small range because the excessive stator-blade temperature required a consistently maximum coolant-flow rate. Further increases in the flow rate were impossible without alteration to the coolant system. For comparison, McAdam's compilation (reference 8) of the data of other investigations for fully developed laminar flow of heated liquids through stationary tubes is shown. A mean through the stator data deviated 15 percent from these investigations. The average curve for the laminar flow of heated and cooled liquids through stationary tubes is also shown.

Coolant pumping power. - The experimental coolant pumping power for various coolant flows is presented in figure 11. The ideal total coolant pumping power calculated by equation (8) for assumed negligible velocity at the rotor inlet is compared with the corresponding experimental power in figure 12. The experimental results are 70 percent larger than the theoretically calculated results at a flow of 8 gallons per minute and a turbine speed of 14,000 rpm. At the same speed, but at a flow of 2 gallons per minute, the experimental results were 50 percent larger than the theoretical results. This discrepancy is probably due to three things: (1) the coolant leakage at the rotor inlet, which results in part of the coolant being pumped to a larger final radius; (2) the error involved in obtaining the wattmeter readings from which the horsepower was calculated; and (3) frictional resistance, particularly in the inlet and outlet passages. The frictional resistance could not be determined because of the variable nature of the other conditions. An idea of the magnitude of the coolant pumping power for this turbine in terms of power output can be obtained by extrapolating the experimental curve for the flow of 8 gallons per minute to a turbine speed of 17,000 rpm (design speed); this extrapolation results in a pumping power of about 30 horsepower. This value is not considered excessive, inasmuch as it is only 2 percent of the calculated turbine power output at design conditions.

General operating results. - Typical operating points similar to those for the aluminum turbine are given in table II. Points of similar mass flow and turbine speed were chosen. Several coolant-flow rates were selected for different inlet-gas temperatures. The average inside heat-transfer coefficients lacked a definite trend because of an appreciable scatter in the turbine data.

At a stator inlet-gas temperature of 1250° F, doubling the coolant flow resulted in an appreciable decrease in the average blade temperature but not in the maximum blade temperature. A further

comparison with runs of a higher coolant flow was not made because of the coolant leakage. The maximum gas temperature of 1740° F resulted in a maximum measured blade temperature of 870° F and an average blade temperature of 350° F at a coolant-flow ratio of 0.175. Because the blade-metal temperatures are so much lower than the gas temperature, the steel turbine shows promise for future operation at higher gas temperature and the potentialities of liquid cooling seem to be amply justified.

A typical blade-temperature distribution around the blade tip is shown in figure 13. The runs plotted were taken from table II and were chosen to give the maximum spread in inlet-gas temperature and several coolant-flow rates. Rotor leakage, particularly at the higher coolant-flow ratios, probably affected these temperatures. The peripheral temperature distribution around the blade tip is presented because the blade temperatures were the highest around this section of the blade and represent the limiting values.

Similar to the data from the aluminum turbine, the blade temperatures decrease with an increase in coolant flow. This trend is indicated by the runs at 1250° F with coolant-flow ratios of 0.057 and 0.131. The maximum blade temperatures occurred at the trailing edge, although at the lower gas temperatures the leading-edge temperatures were also high. At 1250° F and a coolant-flow ratio of 0.131, the leading-edge temperature was only 55° F lower than the trailing-edge temperature. The excessive trailing-edge temperature is best shown at 1740° F where the trailing-edge temperature of 870° F is 430° F higher than the leading-edge temperature.

Comparison of figure 13 with figure 7 indicates that the trend of the temperature distribution around the blade is similar for both the stainless-steel and the aluminum turbines. The temperature decreases from the leading edge toward the center of the blade and then increases rapidly toward the trailing edge. Any conclusions based upon a comparison between the blade-temperature distribution of the two turbines must be tempered by several considerations. The material thermal conductivity differs considerably for the two turbines and may contribute to the higher blade temperatures obtained on the steel turbine. Several significant differences exist, however, between the two turbines that probably affect the temperature distribution as much as the material conductivity, such as blade configuration, method of rotor-coolant circulation, and rotor-coolant leakage in the steel turbine.

Practical considerations. - Preliminary operation of this turbine has revealed several problems in the design of liquid-cooled turbines. Leakage occurred at the point where the coolant was introduced to the rotor and where it was discharged. The coolant was discharged into an annular collector through passages drilled into a projecting lip of the rotor as shown in figure 8(a). A labyrinth seal was provided. The leakage around the labyrinth seal was quickly eliminated by providing additional water outlets at the bottom of the water collector; a reverse thread was cut into the collector to replace the original labyrinth. Leakage at the rotor inlet was more difficult to eliminate, but the situation was improved by the following remedies: Instead of introducing the coolant into the cavity between the rotor and the bolted plate in the form of two jets that had no tangential component, the positions of the jet nozzles were changed to give the jets an appreciable tangential-velocity component. Also, the jet-nozzle-outlet areas were reduced to increase the jet velocity and thereby further increase this component. In addition, vanes were welded to the underside of the water-slinger plate to facilitate the entrance of the coolant into the rotor. No leakage was experienced with the welded steel plugs at the top of the blade cooling passages.

Another difficulty encountered was overheating along the trailing edge of the stator blade, which was in many cases 1000° F or almost double that of the integrated blade temperature. The trailing-edge passage was the smallest and was located as close to the trailing edge (11/64 in.) as the minimum wall thickness for drill drift would allow. The flow distribution through the coolant passages in the original blade showed that only 2.7 percent of the total coolant flow through a blade went through the trailing-edge passage. The flow through the remaining holes was distributed so that 14.3 percent passed through the next smallest hole, and the remaining 83 percent was divided equally among the three largest holes. Some of these difficulties may be alleviated by elongating the trailing-edge holes as shown in figure 14(a). Stress considerations will probably limit such an application to stationary stator blades. The effect of elongating the trailing-edge hole is twofold. The effective length of the uncooled part of the trailing edge is reduced, and the increased cross-sectional area of the cooling passage will result in a more equalized coolant-flow distribution throughout the blade. For instance, calculations made for a proposed blade such as the one in figure 14(a) indicated that 11 percent of the total flow can be expected to pass through the trailing-edge passage and 19.4 percent, through the passage next to it; the remaining 69.6 percent would be equally divided among the three leading-edge passages. The use of a material with a high thermal conductivity would also be helpful in reducing excessive trailing-edge temperatures.

SUMMARY OF RESULTS

An investigation of two water-cooled turbines, one an aluminum turbine utilizing the principle of forced-convection cooling and the other, a stainless-steel turbine utilizing the principle of natural-convection cooling, made to obtain heat-transfer and general operating data, gave the following results:

Forced-Convection Water-Cooled Aluminum Turbine

1. The outside or gas-to-blade heat-transfer data for the rotor blades showed agreement within 10 percent for the range covered with static cascade investigations. The inside or blade-to-coolant heat-transfer data also showed agreement within 40 percent with the data of other investigators for fully developed laminar flow of heated fluids through stationary tubes.

2. The coolant pumping power coincided with theoretical curves calculated on the basis of rate of change of the moment of momentum of the coolant.

3. The maximum blade temperature measured was 405° F at a gas temperature of 1000° F and occurred at the trailing edge. Trailing-edge temperatures always exceeded all other blade temperatures.

4. No difficulty was experienced with coolant leakage either at the blade tip or at the rotor inlet and outlet.

Natural-Convection Water-Cooled Stainless-Steel Turbine

1. The inside or blade-to-coolant heat-transfer data for the rotor blades indicated agreement with the general law describing natural-convection heat transfer; that is, Nusselt number is a function of Grashof and Prandtl numbers. A mean through the inside heat-transfer data for the stator blades with forced-convection cooling showed agreement within 15 percent with the data of other investigators for fully developed laminar flow of heated fluids through stationary tubes.

2. Variations in the readings, coolant leakage, and frictional resistance in the passages probably caused the experimental values of the coolant pumping power to exceed considerably those calculated on the basis of rate of change of the moment of momentum of the coolant.

3. Rotor-blade temperatures were not excessive; the average blade temperature was 350° F at the maximum operating gas temperature of 1740° F for a coolant-flow ratio of 0.175. The maximum rotor-blade temperature always occurred at the trailing edge, being 870° F for the point described. Stator-blade trailing-edge temperatures were excessive (up to 1000° F) and limited turbine operation.

4. Considerable difficulty was experienced with leakage of the rotor coolant.

Lewis Flight Propulsion Laboratory,
National Advisory Committee for Aeronautics,
Cleveland, Ohio.

APPENDIX - SYMBOLS

The following symbols are used in this report:

A	area, sq ft
a,b,n	exponents
C	constant
c_p	specific heat at constant pressure, Btu/(lb)($^\circ$F)
D	diameter, or characteristic dimension, ft
G	weight flow per unit area $\frac{w}{A}$, lb/(sec)(sq ft)
Gz	Graetz number $\frac{w_l c_p}{kL}$
Gr	Grashof number $\frac{L^3 \rho^2 \beta\omega^2 r\Delta T}{\mu^2}$
g	ratio of absolute to gravitational unit of mass, lb/slug, or acceleration due to gravity, ft/sec^2
H	heat-transfer coefficient, Btu/($^\circ$F)(sq ft)(sec)
J	mechanical equivalent of heat, 778.3 ft-lb/Btu
k	thermal conductivity, Btu/($^\circ$F)(ft)(sec)
L	characteristic length of cooling passages, ft
N	turbine speed, rpm
Nu	Nusselt number $\frac{HD}{k}$ or $\frac{HL}{k}$
P	power, hp
Pr	Prandtl number $\frac{c_p \mu g}{k}$
Q	heat flow, Btu/sec
Re	Reynolds number $\frac{\rho VD}{\mu}$ or $\frac{GD}{\mu g}$

r	radius, ft
T	static temperature, ^{o}R
V	absolute fluid velocity, ft/sec
W	relative gas velocity at rotor-blade inlet, ft/sec
w	weight flow, lb/sec
β	coefficient of thermal expansion, $1/^{o}R$
Λ	recovery coefficient (0.85)
μ	absolute viscosity, slugs/(ft)(sec)
ρ	mass density, slugs/cu ft
ω	angular velocity, radians/sec

Subscripts:

av	average
B	blade
e	effective
g	combustion gas
i	inside blade surface
l	liquid
o	outside blade surface
P	pumping
2	blade midsection
3	blade tip
4	disk rim (exposed peripheral section between blades)
5	coolant inlet
6	coolant outlet

REFERENCES

1. Ellerbrock, Herman H., Jr., and Ziemer, Robert R.: Preliminary Analysis of Problem of Determining Experimental Performance of Air-Cooled Turbine. I - Methods for Determining Heat-Transfer Characteristics. NACA RM E50A05, 1950.

2. Ellerbrock, Herman H., Jr.: Preliminary Analysis of Problem of Determining Experimental Performance of Air-Cooled Turbine. II - Methods for Determining Cooling-Air-Flow Characteristics. NACA RM E50A06, 1950.

3. Kottas, Harry, and Sheflin, Bob W.: Investigation of High-Temperature Operation of Liquid-Cooled Gas Turbines. I - Turbine Wheel of Aluminum Alloy, a High-Conductivity Non-strategic Material. NACA RM E8D12, 1948.

4. Meyer, Gene L.: Determination of Average Heat-Transfer Coefficients for a Cascade of Symmetrical Impulse Turbine Blades. I - Heat Transfer from Blades to Cold Air. NACA RM E8H12, 1948.

5. Ellerbrock, Herman H., Jr., and Schafer, Louis J., Jr.: Application of Blade Cooling to Gas Turbines. NACA RM E50A04, 1950.

6. Sieder, E. N., and Tate, G. E.: Heat Transfer and Pressure Drop of Liquids in Tubes. Ind. and Eng. Chem. (Ind. ed.), vol. 28, no. 12, Dec. 1936, pp. 1429-1435.

7. Andrews, S. J., and Bradley, P. C.: Heat Transfer to Turbine Blades. Memo. No. M.37, Nat. Gas Turbine Establishment, M.A.P. (London), Oct. 1948.

8. McAdams, William H.: Heat Transmission. McGraw-Hill Book Co., Inc., 2d ed., 1942.

9. Boelter, L. M. K., Young, G., and Iversen, H. W.: An Investigation of Aircraft Heaters. XXVII - Distribution of Heat-Transfer Rate in the Entrance Section of a Circular Tube. NACA TN 1451, 1948.

TABLE I - TYPICAL OPERATING POINTS FOR WATER-COOLED ALUMINUM TURBINE

Rotor inlet-gas temperature (°F)	Turbine speed (rpm)	Turbine gas flow (lb/hr)	Rotor-coolant flow (lb/hr)	Coolant-flow ratio	Average rotor-blade temperature (integrated around blade mid-section) (°F)	Maximum rotor-blade temperature (trailing edge) (°F)	Rotor-inlet total pressure (in. Hg abs.)	Turbine pressure ratio (total/static)	Rotor outside-heat-transfer coefficient (Btu/(°F)(sq ft)(sec))	Rotor inside heat-transfer coefficient (Btu/(°F)(sq ft)(sec))	Heat to coolant/total heat of fuel (percent)
600	11,430	6870	231	0.034	228	272	23.9	1.67	0.0174	0.139	1.8
			456	.066	200	256			.0224	.240	2.6
			745	.108	184	243			.0228	.280	2.7
		9440	329	0.035	225	279	32.0	1.60	0.0261	0.230	2.1
			469	.050	208	265			.0276	.273	2.4
			930	.099	185	245			.0289	.330	2.6
1000	13,500	5000	780	0.156	242	360	20.8	1.60	0.0201	0.296	3.5
			1550	.310	219	339			.0208	.339	3.7
			2280	.456	210	327			.0217	.371	3.9
		5820	815	0.140	262	386	23.5	1.61	0.0223	0.280	3.4
			1210	.208	237	363			.0236	.343	3.7
			2660	.450	230	357			.0247	.356	3.9
[1]2000	19,000	4140	2250	0.544	---	---	27.5	1.60	------	-----	5.1

[1]Data from reference 3.

TABLE II - TYPICAL OPERATING POINTS FOR WATER-COOLED STAINLESS-STEEL TURBINE

Stator inlet-gas temperature (°F)	Turbine speed (rpm)	Turbine gas flow (lb/hr)	Rotor-coolant flow (lb/hr)	Coolant-flow ratio	Average rotor-blade temperature (integrated over blade surface) (°F)	Maximum rotor-blade temperature (trailing edge) (°F)	Stator-inlet total pressure (in. Hg abs.)	Turbine pressure ratio (total/static)	Rotor inside heat-transfer coefficient (Btu/(°F)(sq ft)(sec))	Heat to coolant/total heat of fuel (percent)
700	14,000	25,200	1430	0.057	172	335	33.5	1.61	0.078	0.28
			3000	.119	167	335	33.3	1.60	.072	.25
1050			1430	0.057	332	500	35.4	1.63	0.115	1.04
			3000	.119	233	---	37.4	1.62	.114	.57
1250			1430	0.057	425	670	38.7	1.63	0.135	1.26
			3300	.131	330	640	38.2	1.63	.149	1.24
1430			3520	0.140	354	660	39.3	1.59	0.159	1.28
1740		15,120	2650	0.175	350	870	31.5	1.21	-----	1.45

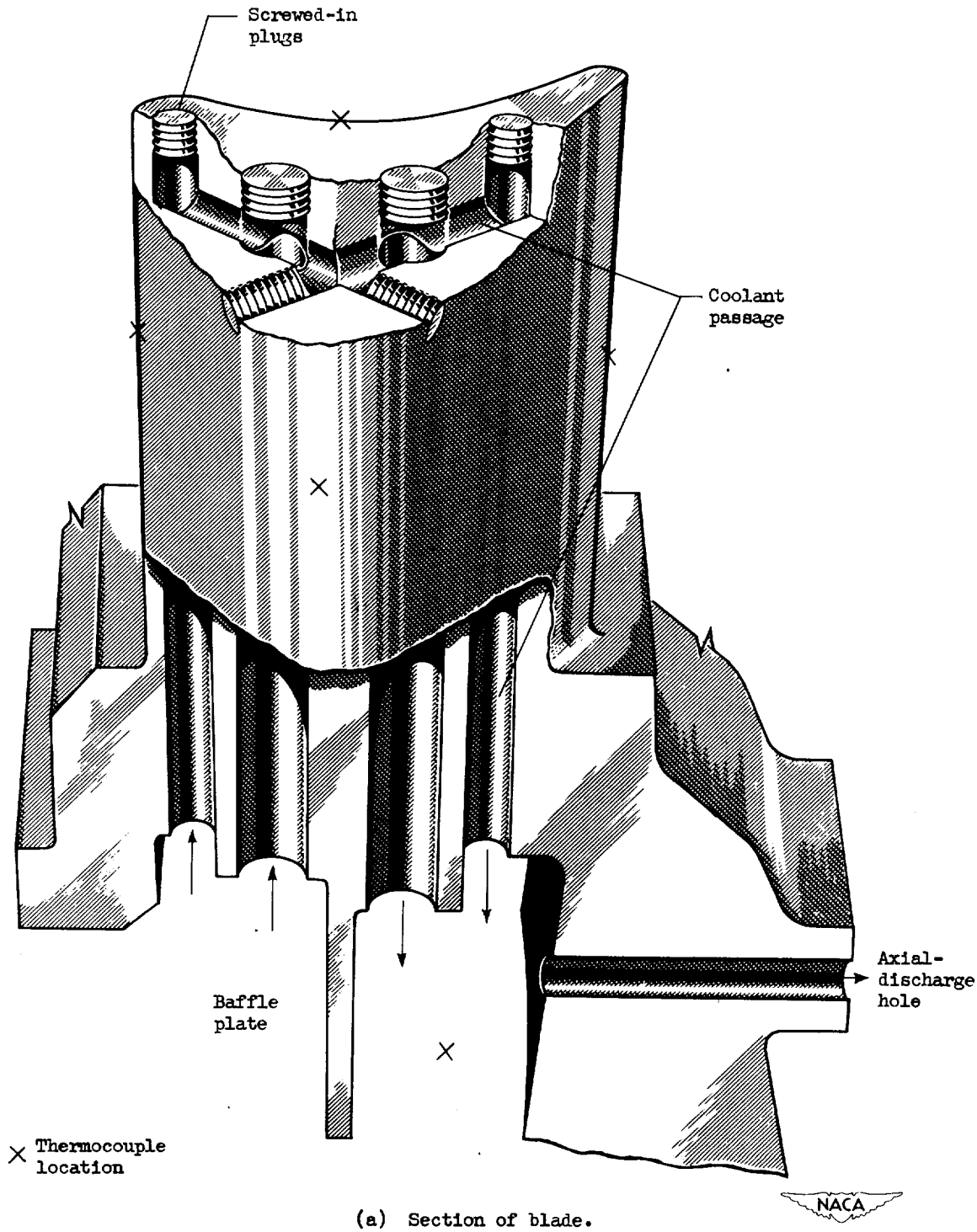

(a) Section of blade.

Figure 1. - Forced-convection water-cooled aluminum turbine.

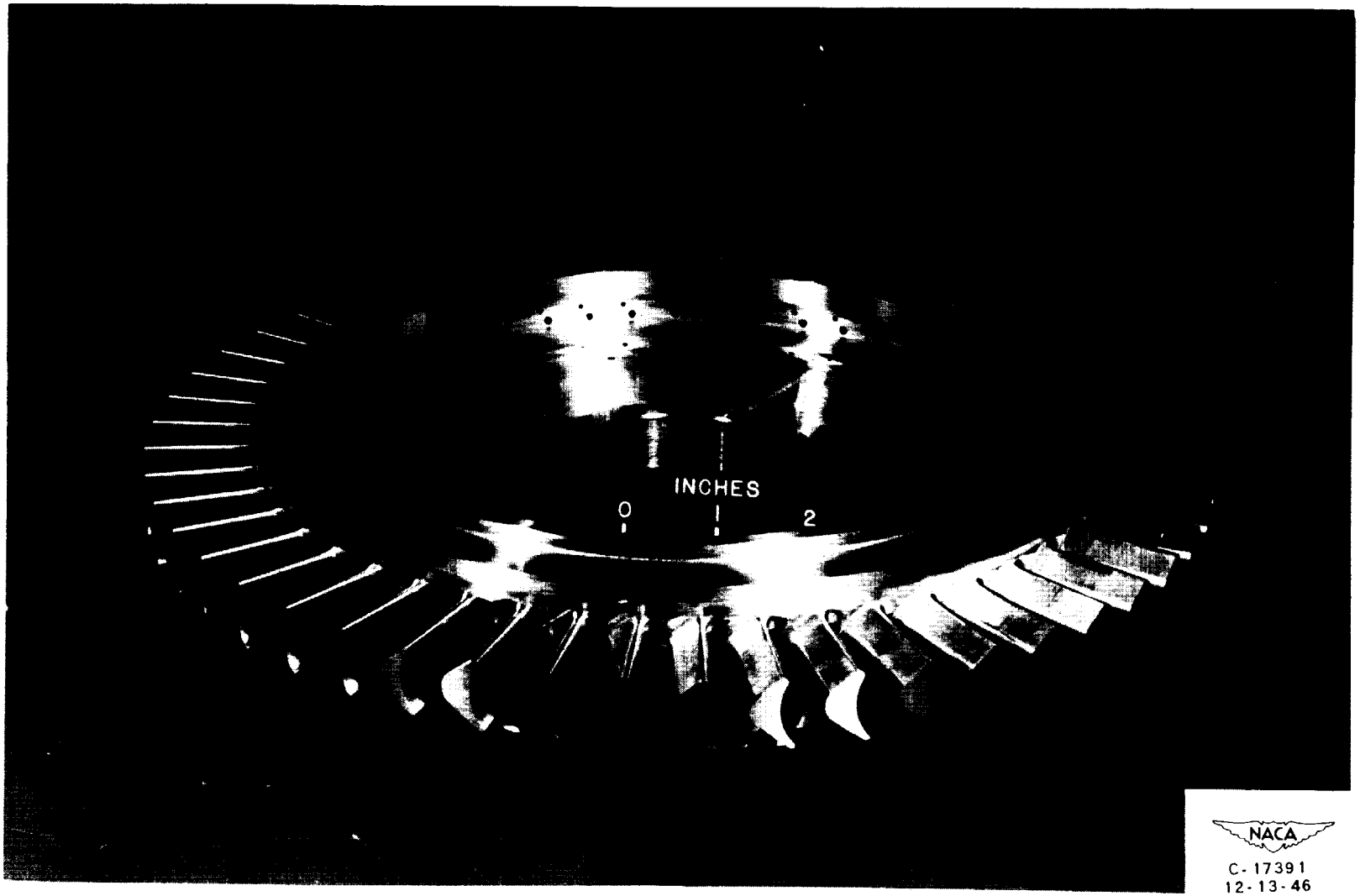

(b) Disk.

Figure 1. - Continued. Forced-convection water-cooled aluminum turbine.

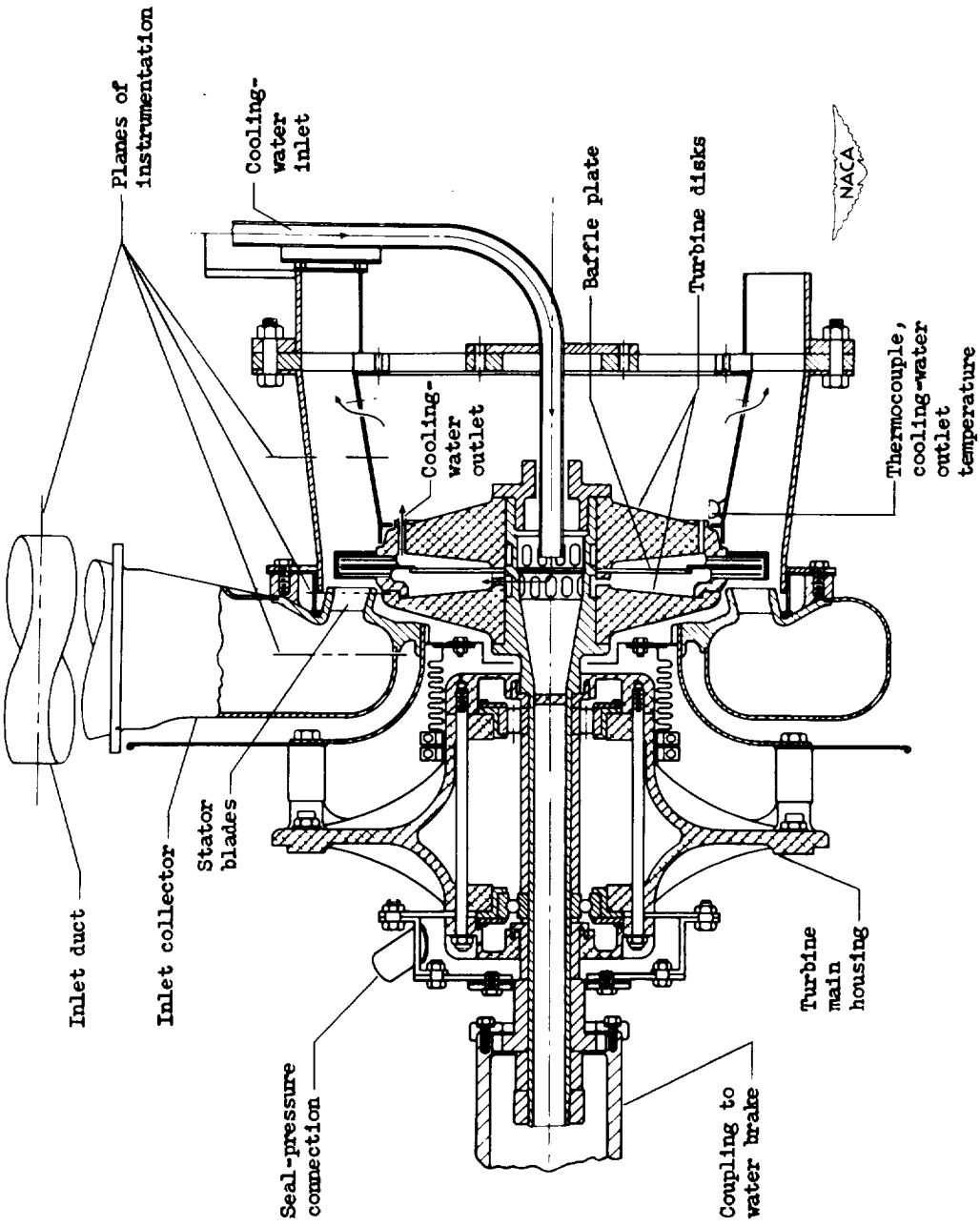

(c) Cross section of installation.

Figure 1. - Concluded. Forced-convection water-cooled aluminum turbine.

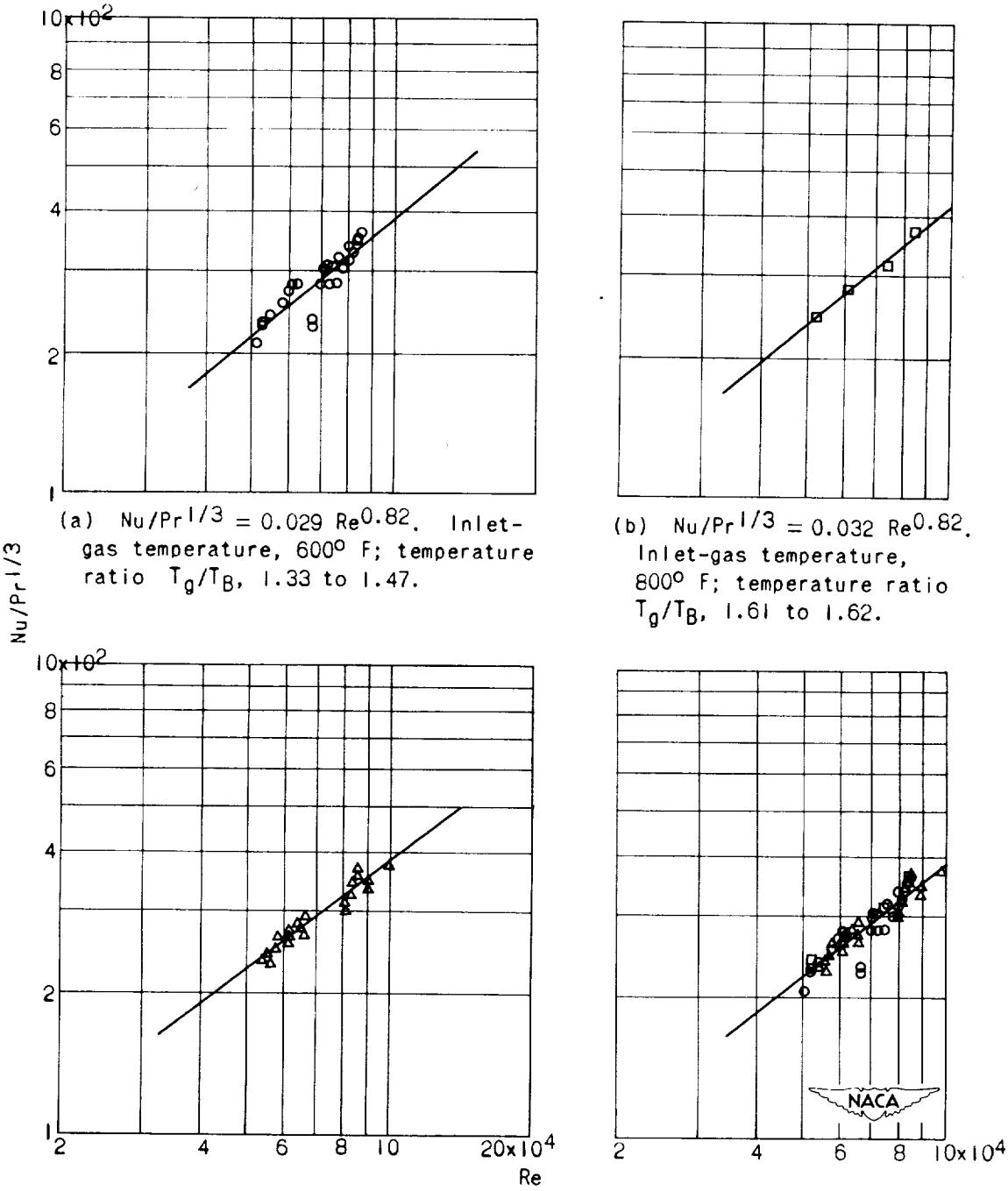

(a) $Nu/Pr^{1/3} = 0.029\ Re^{0.82}$. Inlet-gas temperature, 600° F; temperature ratio T_g/T_B, 1.33 to 1.47.

(b) $Nu/Pr^{1/3} = 0.032\ Re^{0.82}$. Inlet-gas temperature, 800° F; temperature ratio T_g/T_B, 1.61 to 1.62.

(c) $Nu/Pr^{1/3} = 0.057\ Re^{0.76}$. Inlet-gas temperature, 1000° F; temperature ratio T_g/T_B, 1.80 to 1.92.

(d) $Nu/Pr^{1/3} = 0.047\ Re^{0.78}$. Data from all runs.

Figure 2. - Outside heat-transfer data from forced-convection water-cooled aluminum rotor blades. Fluid properties of gas based on blade-wall temperature; velocity taken at rotor inlet.

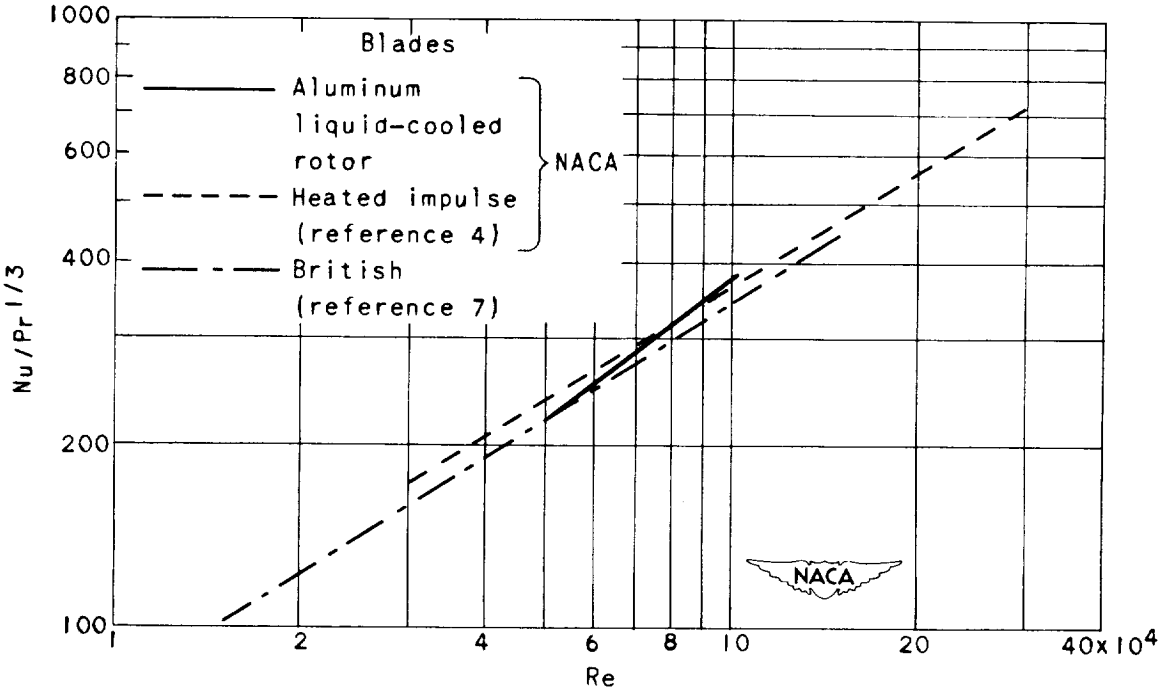

Figure 3. - Comparison of outside heat-transfer data from forced-convection water-cooled aluminum turbine with results from static cascades.

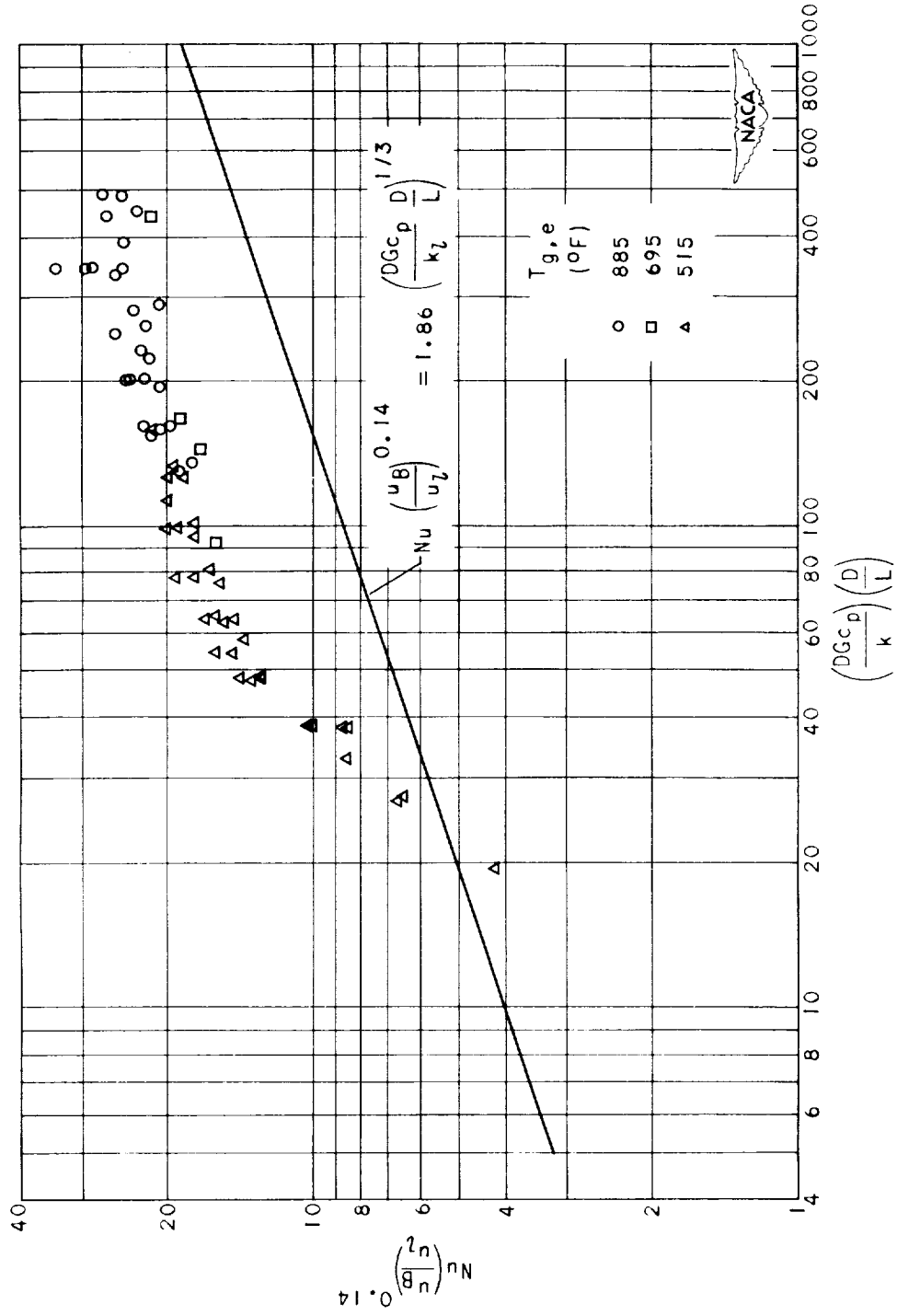

Figure 4. - Comparison of inside heat-transfer data from forced-convection water-cooled aluminum turbine with equation in reference 6 for fully developed laminar flow of heated and cooled liquids inside stationary tubes. Fluid properties based on average coolant temperatures.

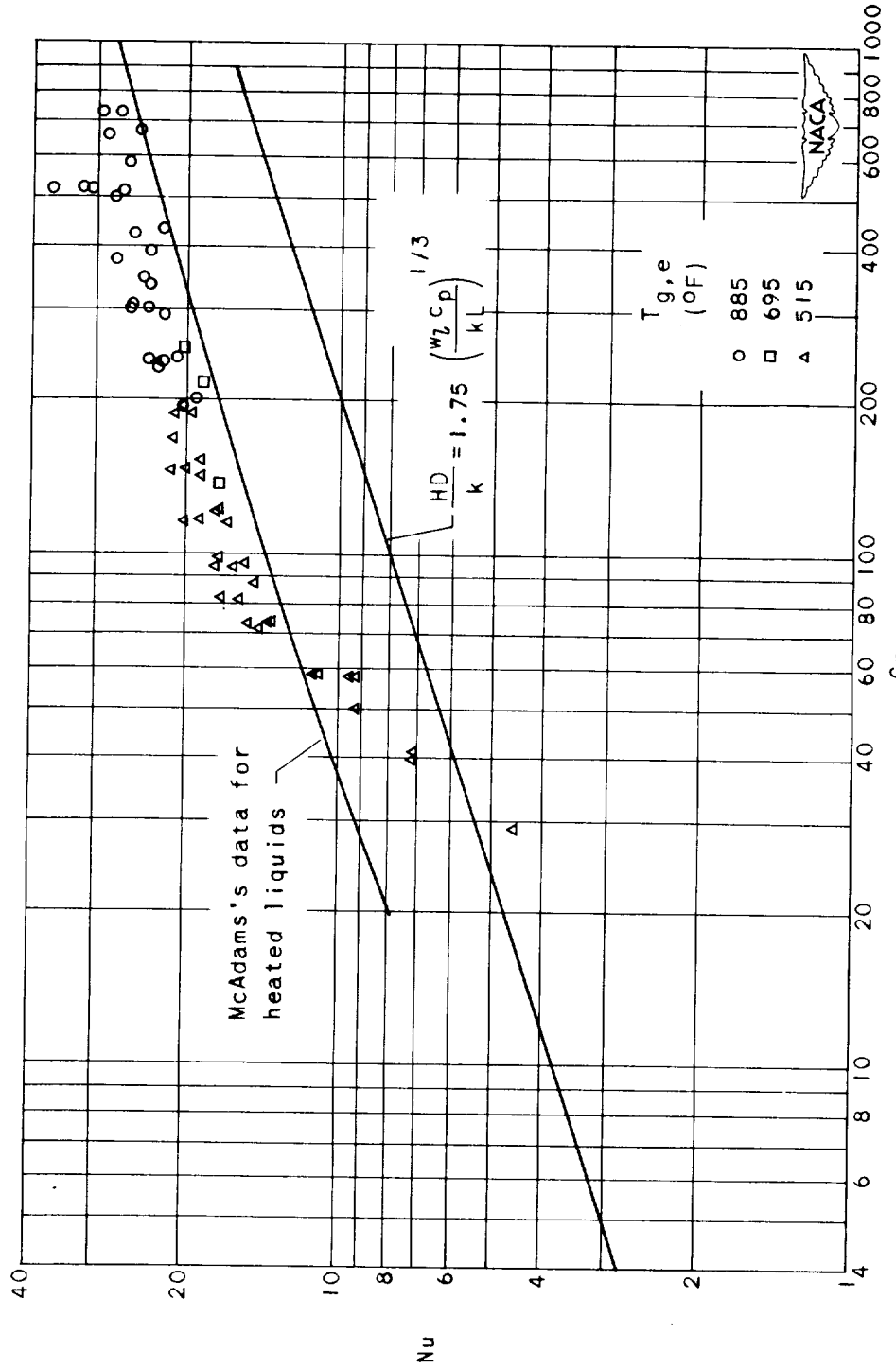

Figure 5. - Comparison of inside heat-transfer data from forced-convection water-cooled aluminum turbine with data and equation in McAdams (reference 8) for fully developed laminar flow of heated and cooled liquids inside stationary tubes. Fluid properties based on average coolant temperatures.

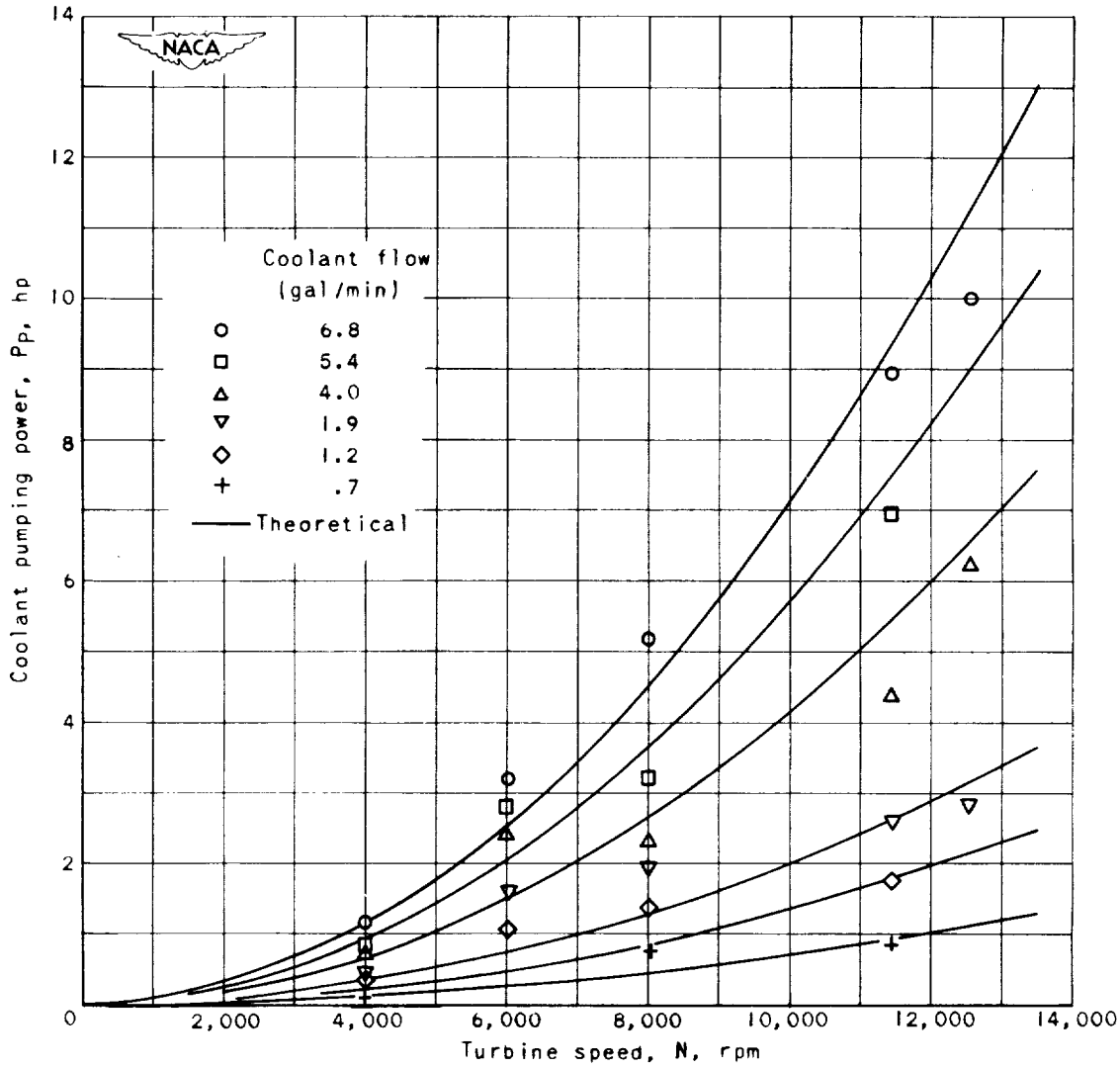

Figure 6. – Comparison of experimental coolant pumping power for forced-convection water-cooled aluminum turbine with coolant pumping power calculated on basis of rate of change in moment of momentum.

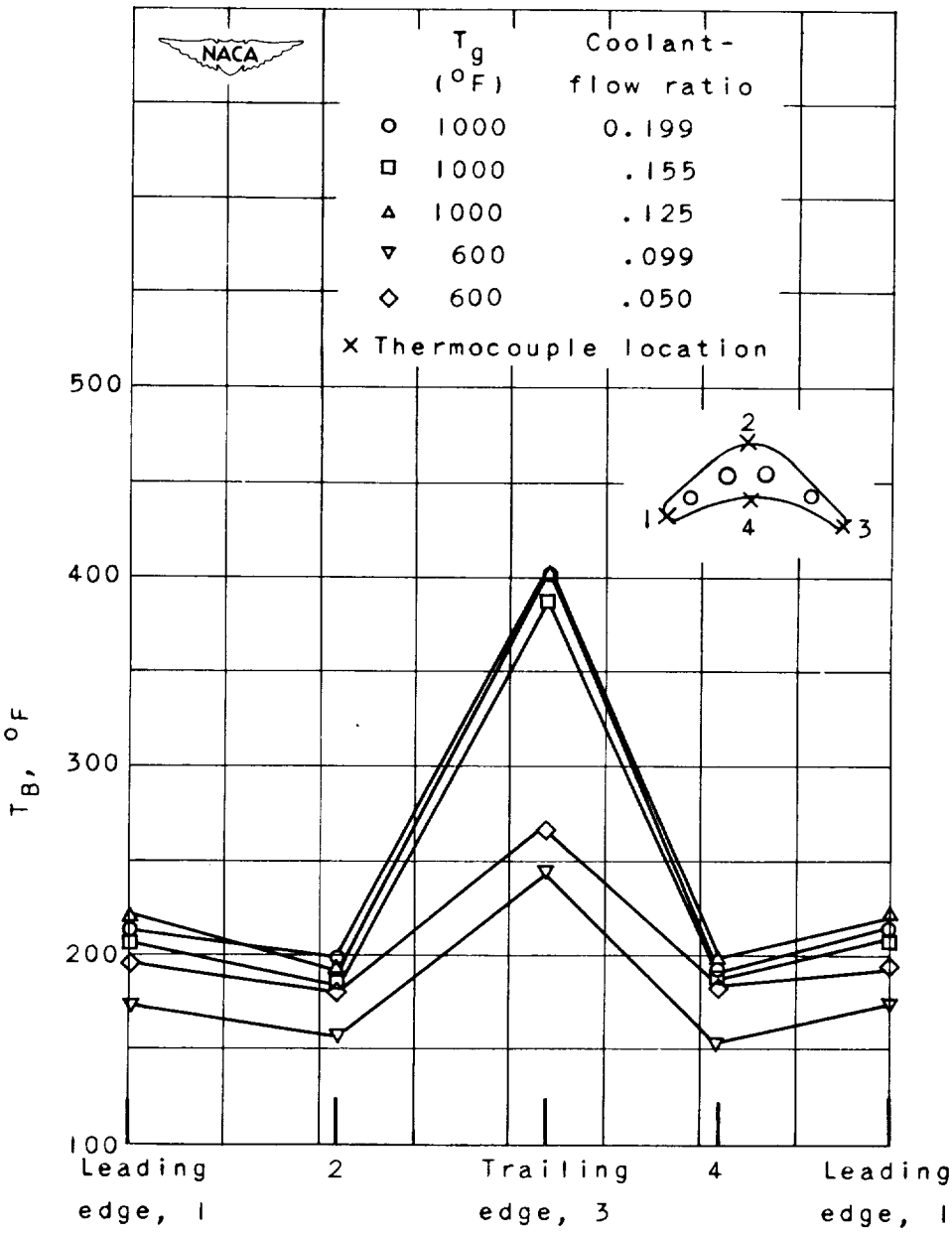

Figure 7. - Midsection-blade temperature distribution for forced-convection water-cooled aluminum turbine.

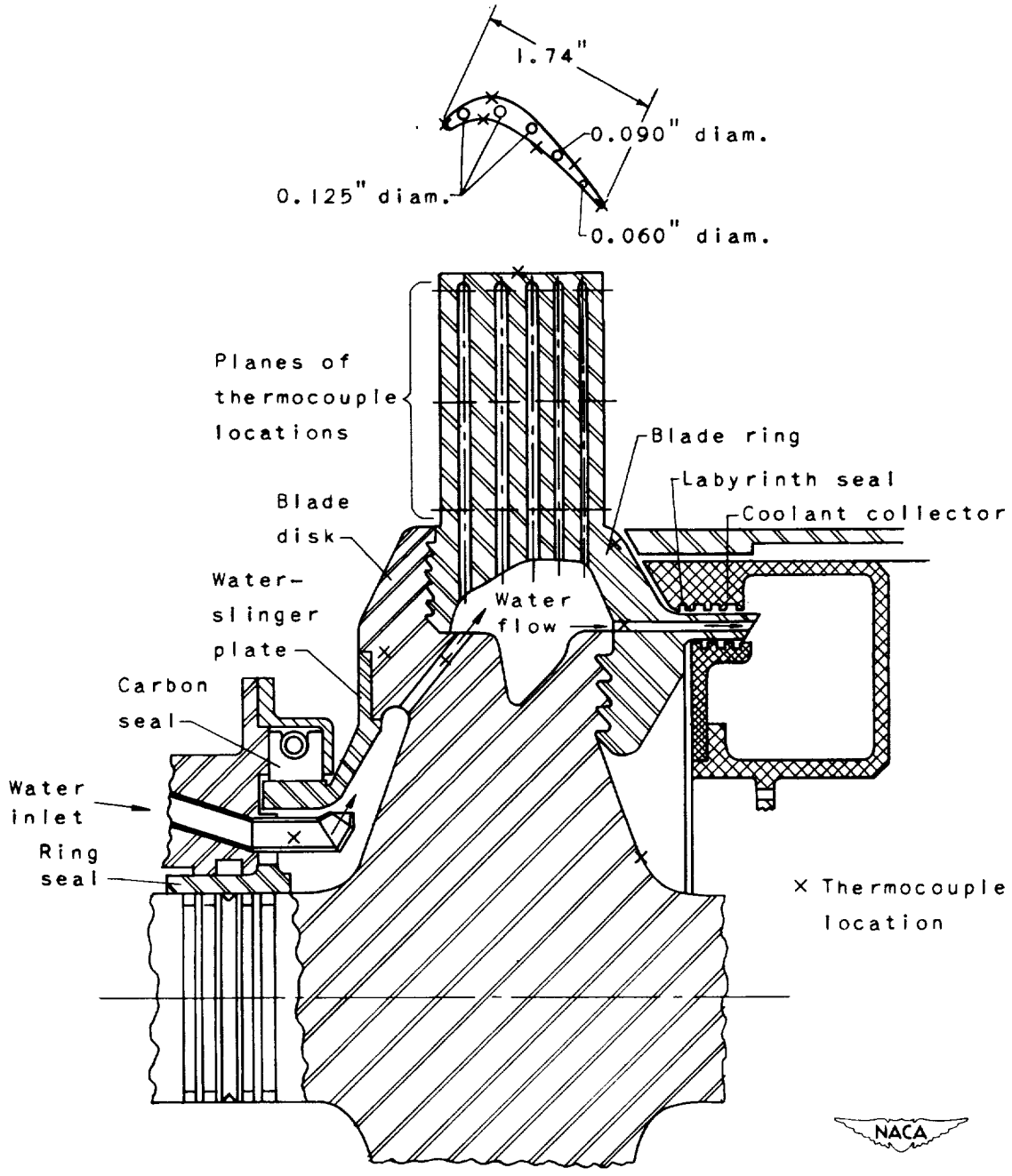

(a) Rotor and coolant system.

Figure 8. - Cross section of natural-convection water-cooled stainless-steel turbine.

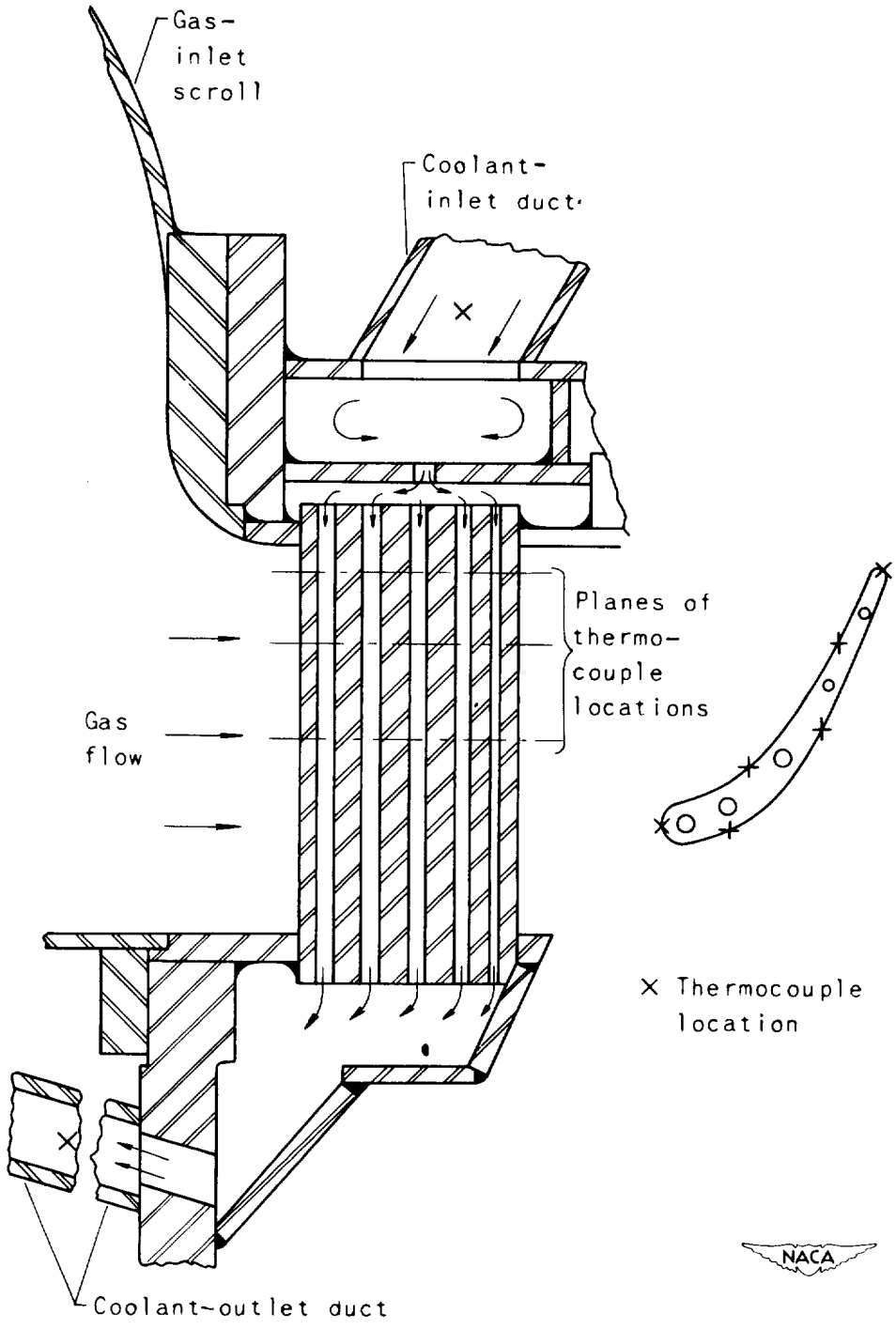

(b) Stator blade and blade mounting.

Figure 8. – Continued. Cross section of natural-convection water-cooled stainless-steel turbine.

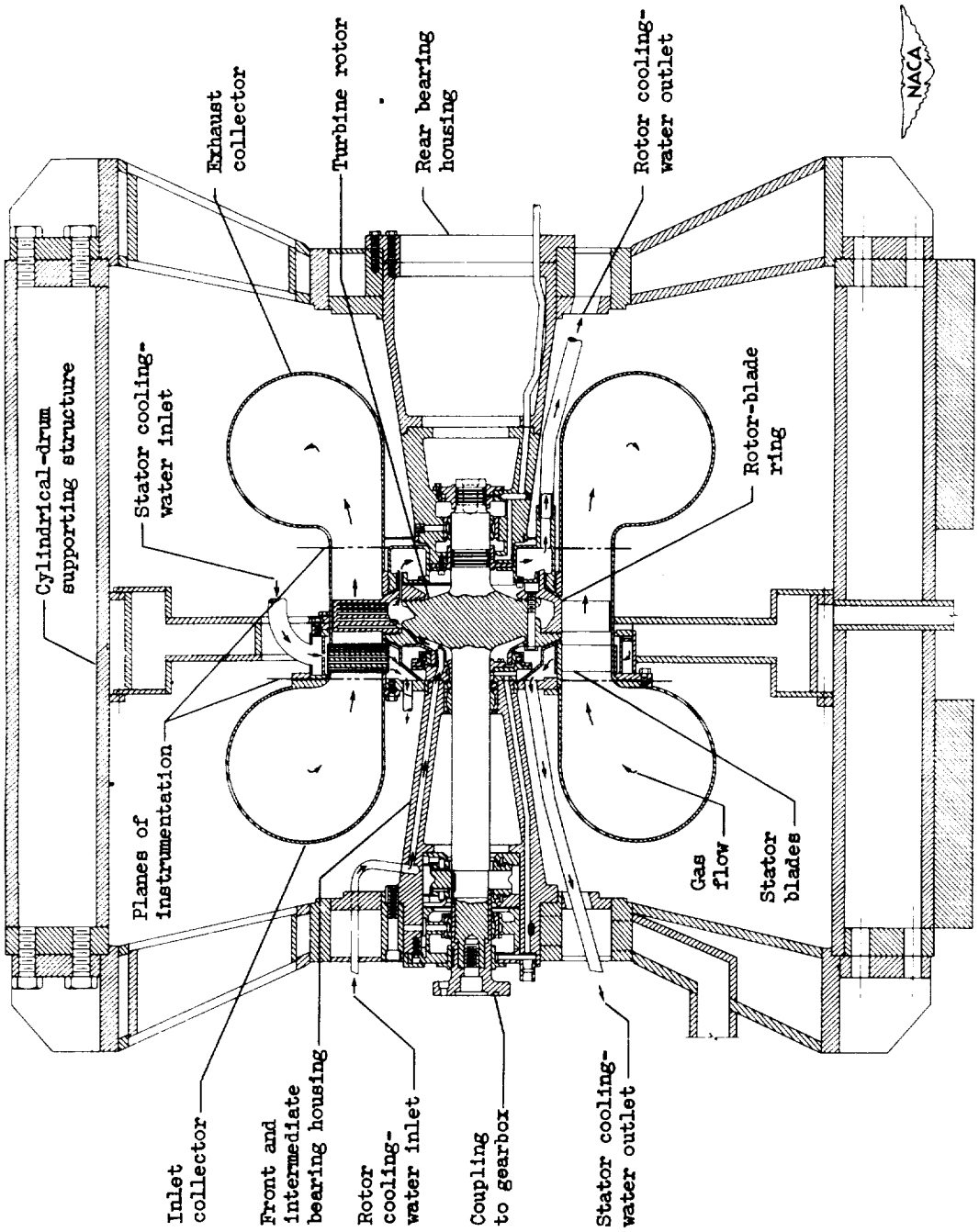

(c) Installation.

Figure 8. - Concluded. Cross-section of natural-convection water-cooled stainless steel turbine.

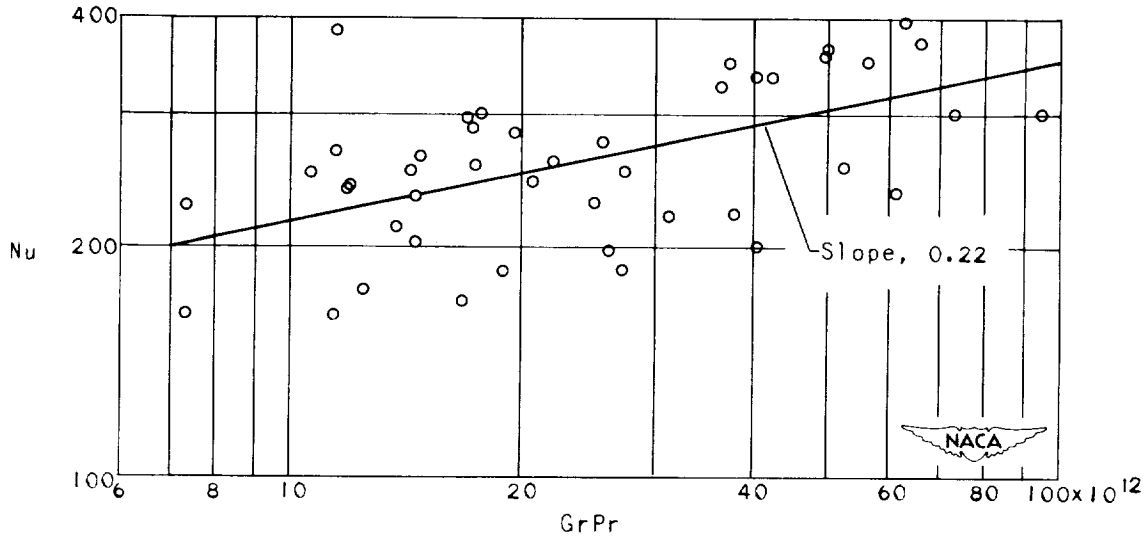

Figure 9. - Inside heat-transfer data from natural-convection water-cooled stainless-steel rotor blades. Fluid properties based on average coolant temperature.

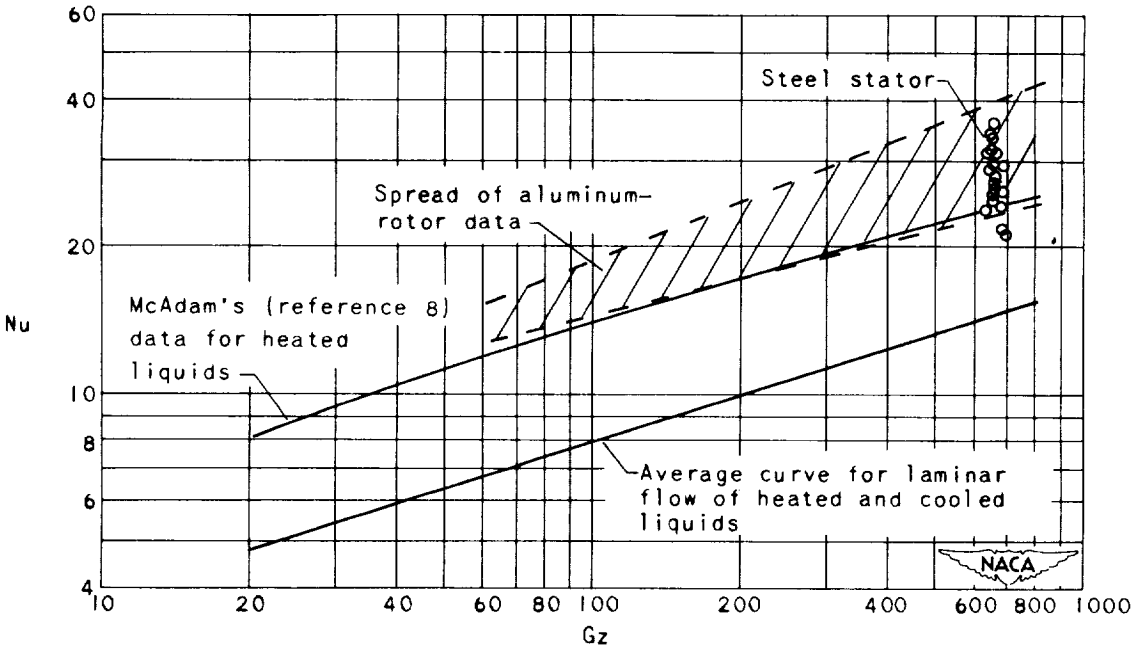

Figure 10. - Comparison of forced-convection inside heat-transfer data. Fluid properties based on average coolant temperature.

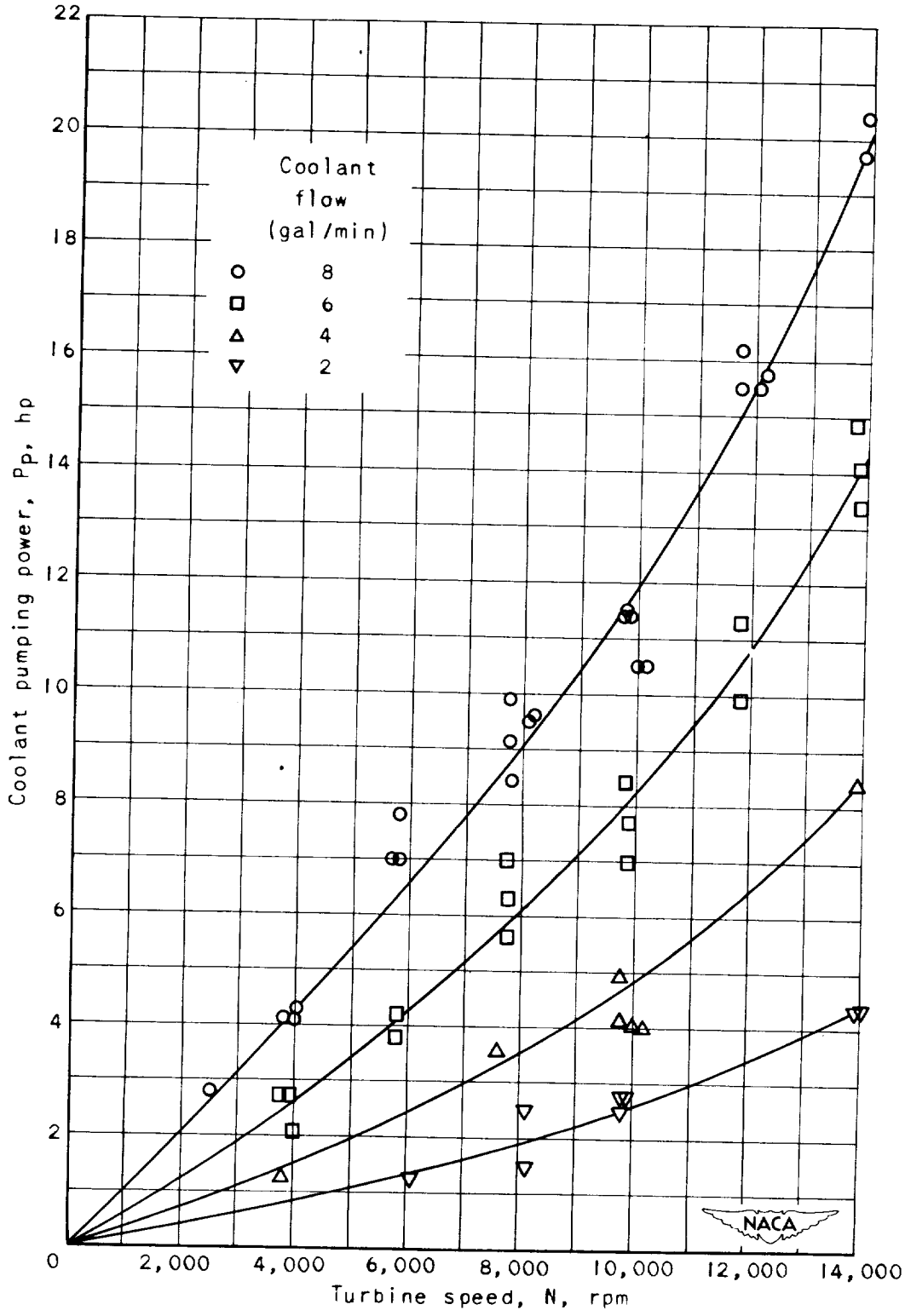

Figure 11. – Experimental coolant pumping power for natural-convection water-cooled stainless-steel turbine rotor.

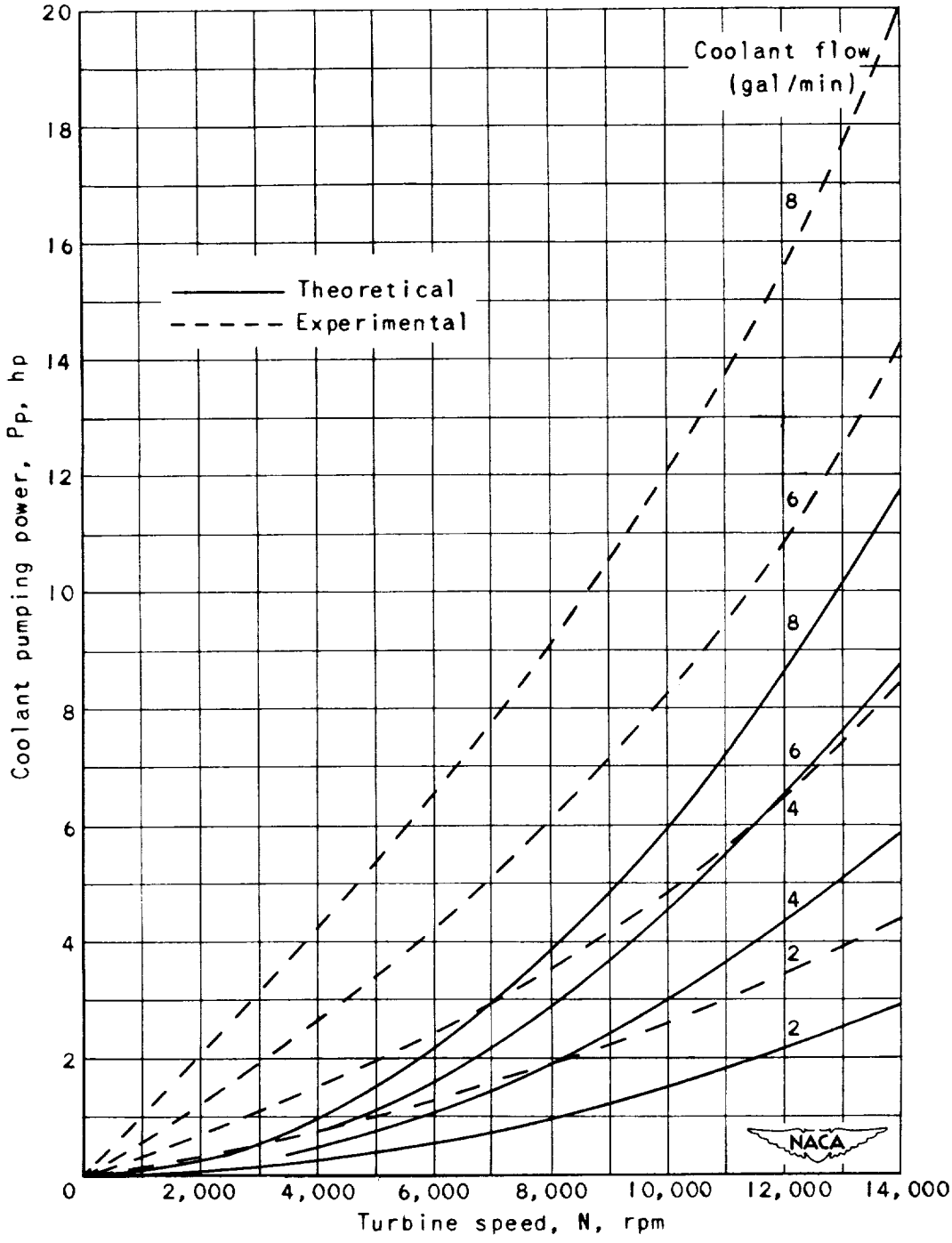

Figure 12. – Comparison of experimental coolant pumping power from natural-convection water-cooled stainless-steel turbine with coolant pumping power calculated by rate of change in moment of momentum.

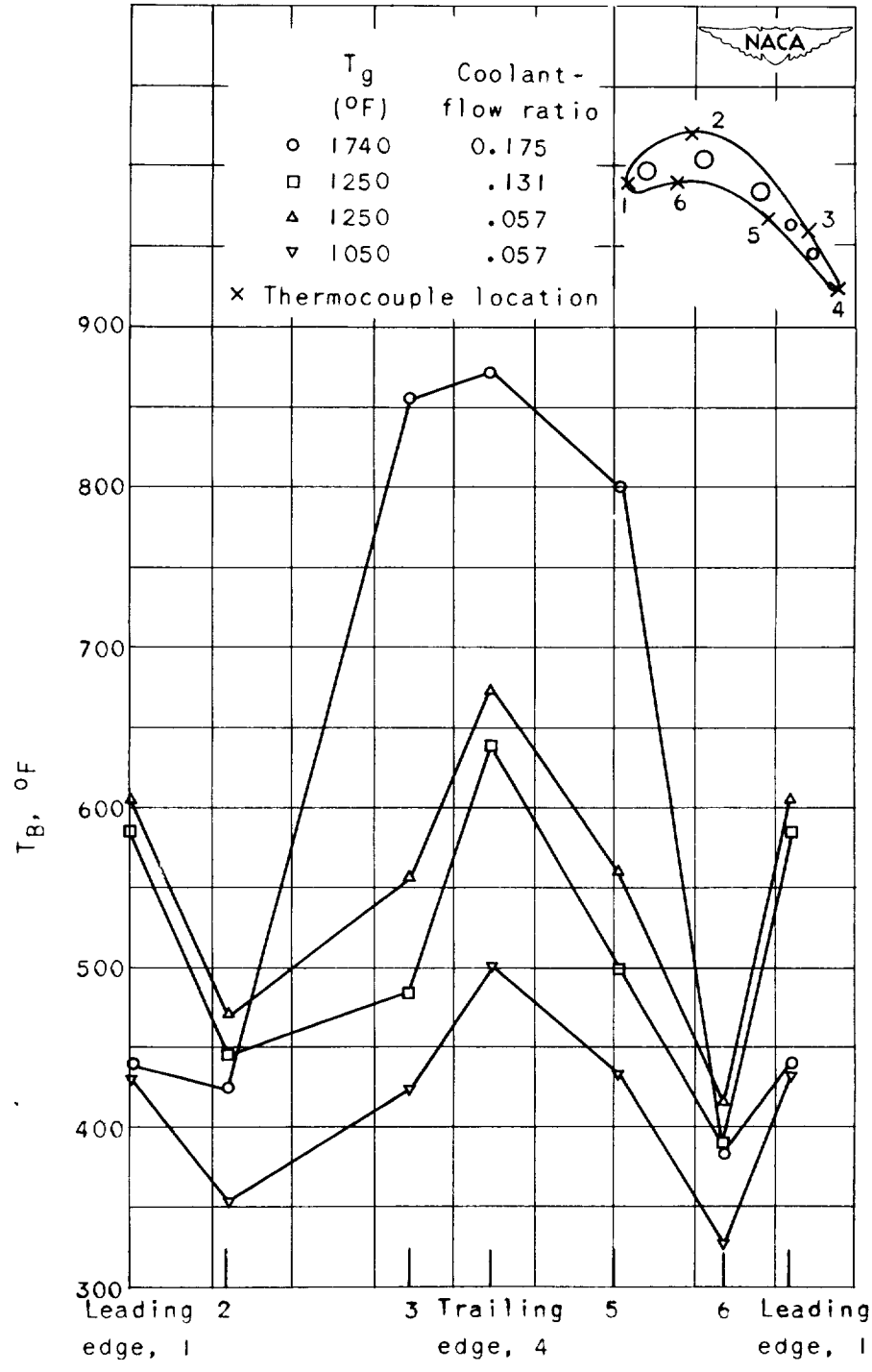

Figure 13. - Temperature distribution at blade tip for natural-convection water-cooled stainless-steel turbine rotor.

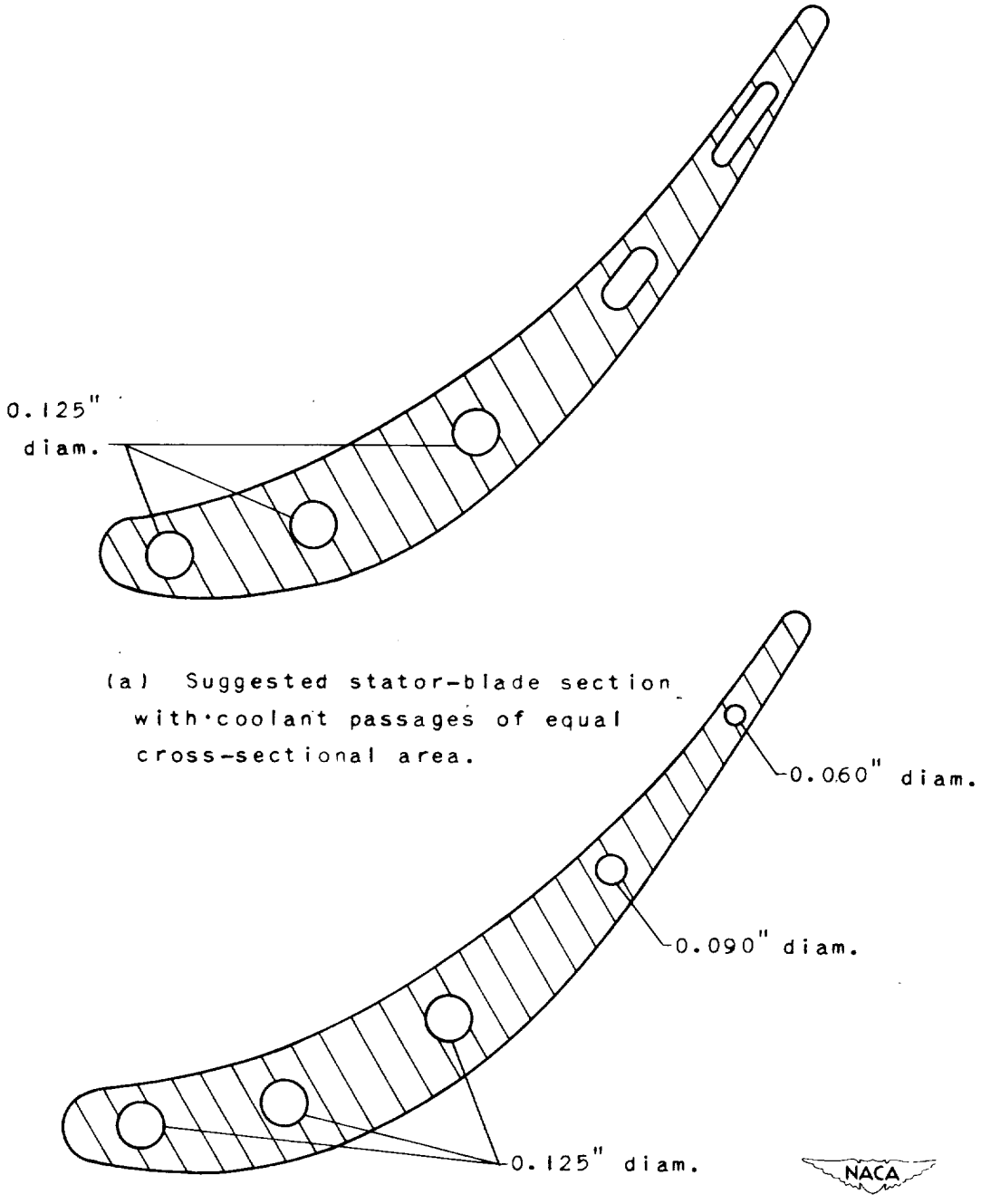

(a) Suggested stator-blade section with coolant passages of equal cross-sectional area.

(b) Original stator-blade section with coolant passages of various diameters.

Figure 14. - Cross section of suggested and original stator blades for natural-convection water-cooled stainless-steel turbine.

NACA-Langley - 6-30-50 250